19930092585 A-71

NATIONAL ADVISORY COMMITTEE FOR AERONAUTICS

WARTIME REPORT

ORIGINALLY ISSUED

August 1945 as
Memorandum Report A5H30

CORRELATION OF WIND-TUNNEL PREDICTIONS WITH FLIGHT TESTS OF A TWIN-ENGINE PATROL AIRPLANE. II - LATERAL- AND DIRECTIONAL-STABILITY AND -CONTROL CHARACTERISTICS

By Noel K. Delany and William M. Kauffman

Ames Aeronautical Laboratory
Moffett Field, California

WASHINGTON

NACA WARTIME REPORTS are reprints of papers originally issued to provide rapid distribution of advance research results to an authorized group requiring them for the war effort. They were previously held under a security status but are now unclassified. Some of these reports were not technically edited. All have been reproduced without change in order to expedite general distribution.

MR No. A5H30

NATIONAL ADVISORY COMMITTEE FOR AERONAUTICS

MEMORANDUM REPORT

for the

Bureau of Aeronautics, Navy Department

CORRELATION OF WIND-TUNNEL PREDICTIONS WITH FLIGHT TESTS OF A TWIN-ENGINE PATROL AIRPLANE. II - LATERAL- AND DIRECTIONAL-STABILITY AND -CONTROL CHARACTERISTICS

By Noel K. Delany and William H. Kauffman

SUMMARY

The lateral- and directional-stability and -control characteristics of a twin-engine patrol airplane as predicted from the results of wind-tunnel tests of a powered model and as measured in flight are compared in this report. The predictions from wind-tunnel-test data were in good agreement with the flight-test results. The results show that such predicted flying-qualities characteristics are sufficiently accurate to indicate the unsatisfactory lateral- and directional-stability and -control characteristics of airplanes in the preliminary design stage. The wind-tunnel data may be used to deduce the chief reasons for these unsatisfactory characteristics and to indicate possible methods of improvement.

INTRODUCTION

During the past several years, the flying qualities of various airplanes have been estimated from the results of wind-tunnel tests made while the airplane was in the design stage. These predicted flying qualities have been used to determine compliance with the critical stability and control requirements. Basic changes to the airplane, necessary for correction of unsatisfactory characteristics, have been determined from these data. No comprehensive study of the

accuracy of such methods of predictions has been made in the past, and it was considered desirable to compare in a detailed manner the predicted flying qualities with those measured in flight. Such a comparison should lead to a better understanding of the accuracy of the predictions, as well as to improvements in tests and methods which will result in more accurate estimates in the future.

As a part of this correlation program, flight tests were made to determine the flying qualities of a low-wing, twin-engine patrol airplane for the purpose of comparison with the results of tests of a 1/9-scale powered model in the Ames 7- by 10-foot wind tunnel. (See reference 1.) The airplane configurations and flight conditions for some of the flight tests were different from those used in the original wind-tunnel tests reported in reference 1; hence, additional wind-tunnel tests were made and the results used in computing the predicted flying qualities presented herein.

For this airplane, lateral- and directional-stability and -control characteristics of importance in design work and most suitable for correlation were those in steady sideslips, asymmetric-power flight, aileron rolls, and rudder rolls; hence, the results presented herein are confined to these characteristics. The correlation of the longitudinal-stability and -control characteristics have been presented in reference 2.

DESCRIPTION OF THE AIRPLANE

The test airplane is a twin-engine, low-wing, medium-size monoplane. It is equipped with retractable conventional-type landing gear, twin-vertical-tail surfaces, and trailing-edge Fowler-type wing flaps. Figures 1(a) and 1(b) are photographs of the airplane as instrumented for the flight tests and figure 2 is a three-view drawing. Figure 3 shows details of the vertical tail surfaces and figure 4 of the wing and aileron. Further information on the vertical tail, wing, and aileron are given in tables I and II. The general specifications and dimensions of the airplane have been presented in reference 2.

The relationship of the rudder-pedal travel and the rudder angle as measured on the ground with no load on the surface is given in figure 5. Each control-surface angle is

defined as the angle between the chord line of the movable surface and the chord line of the surface to which it is attached. The mechanical advantage of the system varied over a small range and the data of figure 5 represent average values. The kinematics of the rudder-tab system, which was a combination trim and boost type, are represented in figure 6. The boost action was adjusted according to the recommendations of reference 3.

The kinematics of the aileron control system, as measured on the ground with no load on the control surfaces, are presented in figure 7. The term "total aileron angle" refers to the algebraic difference between the angles of the two ailerons, and is referred to as "left" when the left aileron is up. The aileron-tab characteristics are shown in figure 8. The right aileron tab acted as a boost tab only and the left aileron tab as a combination boost and trim tab.

The friction in the rudder and aileron control system, as measured on the ground during slow control movements through neutral, was ±25 and ±6.5 pounds, respectively.

DESCRIPTION OF THE MODEL

The 1/9-scale powered model of the airplane (fig. 9) has been described in reference 1. Except for the omission of control-surface tabs, the model was aerodynamically similar to the airplane. The contour and basic dimensions of the model control surfaces, except for the center section of the elevator, matched the full-scale airplane closely.

Rudder hinge moments were measured by means of resistance-type strain gages. The model had only one aileron (left-hand side) which, due to the piano hinge and small scale, could not be equipped with strain gages for measuring hinge moments.

Power was supplied by two electric motors which drove three-blade, right-hand-rotation, 1/9-scale propellers. The propeller-blade angle (30° at the 0.75-radius station) was selected as a good compromise between the high-speed and low-speed power-on flight conditions. In no case did the use of a fixed blade angle lead to serious errors in torque coefficient.

SYMBOLS

The definitions of symbols used in this report are as follows:

δ_r	rudder angle (measured between rudder and vertical-fin chord lines), degrees
δ_a	total aileron angle (algebraic difference of angles of the two ailerons), degrees
F_r	net rudder control force, pounds
F_a	aileron control force (applied tangentially on a 14-inch-diameter wheel), pounds
$C_{h_{\delta_r}}$	rate of change of rudder hinge-moment coefficient with rudder angle $(\partial C_{h_r}/\partial \delta_r)$ (tab zero, sideslip angle constant)
C_{h_β}	rate of change of rudder hinge-moment coefficient with sideslip angle $(\partial C_{h_r}/\partial \beta)$ (tab zero, rudder angle constant)
β	sideslip angle, degrees
Φ	angle of bank, degrees
σ	air density ratio
T_c	thrust coefficient
p	rolling velocity, radian per second
b	wing span, feet
V	true airspeed, feet per second
M.A.C.	wing mean aerodynamic chord, feet

FLIGHT TESTS

A description of the basic configurations for which flight tests were conducted is as follows:

Condition	Position			Power			Approx. indicated stalling speed (mph)
	Flap	Gear	Cowl flap	Manifold pressure (in. Hg)	Engine speed setting (rpm)	Brake horse-power per engine [1]	
Glide	Up	Up	Closed	Throttled	Propeller set in high pitch	--------	106
Climb	Up	Up	Closed	36	2400	1350	84
Landing	Full down (38°)	Down	Closed	Throttled	2400	--------	97
Approach	Full down (38°)	Down	Closed	20	2400	530	85
Wave-off	Full down (38°)	Down	Closed	41.5	2700	1650	76

[1] From engine-performance chart for low-blower gear ratio at 6500 feet.

The average airplane gross weight, corrected for fuel consumption, was approximately 26,500 pounds for all these tests, and the center-of-gravity location was 0.275 M.A.C. (flaps and gear up). The average test pressure altitude was about 6500 feet.

Rudder Rolls

Abrupt aileron-fixed rudder rolls were performed at 150 and 280 miles per hour in the climb condition. The rolls were started from steady straight flight, wings level; while the ailerons were held fixed, an abrupt rudder deflection was applied and held as steady as possible until maximum rolling velocity was attained.

Steady Sideslips

Short records were taken in steady straight flight at various angles of sideslip, left and right, up to the maximum as limited by high rudder forces or tail stalling. Tests were performed at various constant airspeeds in the climb and glide conditions, and at one low airspeed in the landing, approach, and wave-off conditions.

Asymmetric-Power Flight

The effectiveness of the rudder and aileron (tabs set at neutral) in controlling the airplane under asymmetric-power conditions, flaps and gear up, was investigated by performing steady sideslips at various airspeeds while one engine was developing maximum available power and the other engine was throttled. The tests were performed for the right- and left-engine-throttled conditions at about 10-miles-per-hour increments from 170 to 140 miles per hour (the minimum deemed feasible).

Aileron Rolls

Abrupt rudder-fixed aileron rolls were performed at various airspeeds in the climb and landing conditions. While in steady straight flight at each airspeed, various amounts of left and right aileron deflection up to the maximum obtainable were applied and held until maximum rolling velocity was attained.

WIND-TUNNEL TESTS

The procedure for the wind-tunnel tests was the same as that outlined in reference 1, but most of the data presented herein were obtained from repeat tests which have not been reported previously.

Basic Data

The data were obtained from constant-thrust-coefficient yaw tests as described in reference 2. The estimated flight $T_c - C_L$ relationships for the various power conditions were used to determine the operating conditions for the wind-tunnel

tests. The flight thrust and lift coefficients were matched as accurately as possible in all cases. Throttled engine operation with the propeller not feathered (glide, landing, and asymmetric-power conditions) was simulated by operating at a thrust coefficient of -0.04. Asymmetric-power tests were made to simulate both left- or right-engine failures. Aileron-effectiveness data were obtained from previous tests on the model (reference 1), and the aileron hinge moments were estimated from the data of references 4 and 5, corrected by the method of reference 6 for physical differences such as plan form and balance area.

Methods for Predicting Stability and Control Characteristics

The airplane gross weight (26,500 lb), center-of-gravity location (0.275 M.A.C., flaps and gear up), kinematics of the control systems, and boost-tab ratios as measured on the airplane were used in all the computations. The tab effectiveness for the rudder and ailerons was estimated from reference 7.

The rolling and yawing velocities and the sideslip angle in aileron rolls and rudder rolls were computed by the methods outlined in reference 8. The damping coefficients in yaw and roll were estimated from references 9, 10, and 11. No corrections for wing twist were made in the computation of the maximum rolling velocity. The rudder forces in abrupt rudder rolls were computed on the assumption that the maximum rudder force was developed at the instant the maneuver was started. Aileron forces in rolls were corrected for the change in angle of attack due to the rolling velocity.

The characteristics in steady sideslips for both the symmetric- and asymmetric-power conditions were computed by the methods of reference 12.

RESULTS AND DISCUSSION

Characteristics in Rudder Rolls

Data obtained in abrupt aileron-fixed rudder rolls are useful in estimating values of $C_{h_{\delta_r}}$ and in assessing the

dihedral effect. Results are presented in figure 10 in the form of curves of rudder control force and maximum yawing and rolling velocities at sea level plotted against change in rudder angle.

The values of rudder angle are not corrected for stretch in the control system between the surface and the position recorder, except where noted. However, on comparison of the flight and wind-tunnel results, it was found that in some cases this correction was of importance. For instance, additional rudder-force curves corrected for the effect of stretch (approx. 0.005° per lb) are shown in figure 10. It is seen that, although the original flight data indicate lower control forces (hence, $C_{h_{\delta_r}}$) than for the wind tunnel, the corrected curves show higher forces. Values of $C_{h_{\delta_r}}$ for the conditions of figure 10 are approximately -0.0095 for the corrected flight data and -0.0080 for the wind-tunnel tests. The maximum angular velocities are in fair agreement, and corrections for stretch would tend to improve the correlation at the higher speed of 280 miles per hour.

Steady Sideslips

The characteristics in steady sideslips are shown in figures 11 to 15 as a function of sideslip angle for each test condition and airspeed. Both the flight and the wind-tunnel results indicate that the characteristics are satisfactory except for generally high rudder control forces, a tendency toward rudder-force reversal at large angles of right sideslip in low-speed power-on conditions, and marginal control-free dihedral effect at low speeds, flap and gear down.

The rudder-fixed directional stability, as measured by the variation of rudder angle with sideslip $(d\delta_r/d\beta)$, is positive in all cases, and wind-tunnel and flight values of $d\delta_r/d\beta$ compared closely. Most of the difference at high speed (fig. 12) is seen to be due to the effect of stretch.

The rudder-free directional stability, as measured by the variation of rudder control force with sideslip angle $dF_r/d\beta$, indicated by the flight and wind-tunnel results is approximately the same at low airspeeds. The force-reversal tendency with power on (figs. 12(a) and 14) occurs at a smaller angle of right sideslip for the wind-tunnel predictions than for the flight tests, due probably to the earlier partial-flow

breakdown over the vertical tail associated with the lower model Reynolds number. In the landing condition (fig. 13) the wind-tunnel data obtained at the high test lift coefficient ($C_L = 1.70$, near the maximum for the model) and low thrust coefficient were erratic. Recomputed control-force values based on data obtained from tests at the same thrust coefficient but at a lower lift coefficient ($C_L = 1.10$) give better agreement with the flight results. At the higher airspeeds (figs. 11 and 12), the larger rudder control forces for the flight tests arise in part from the greater values of $C_{h_{\delta_r}}$ noted in the rudder-roll discussion. The remainder of the difference can be attributed chiefly to differences in values of C_{h_β}, equal to about -0.0045 for flight tests and -0.0040 for wind-tunnel tests.

The aileron-fixed lateral stability (dihedral effect), as measured by the variation of total aileron angle with sideslip angle is positive in all cases and the agreement between flight and wind-tunnel data is good. The higher value of $d\delta_a/d\beta$ for the flight data at higher speeds (fig. 12) may be due to wing-twist effect.

Positive aileron-free lateral stability, as measured by the variation of aileron control force with sideslip angle, is shown for flap- and gear-up conditions by both the flight and wind-tunnel results, and the values of $dF_a/d\beta$ are in good agreement. For the flap- and gear-down conditions (figs. 13, 14, and 15), marginal stability is indicated by all the data.

The cross-wind force characteristics, as shown by the variation of angle of bank with sideslip angle, are satisfactory in all cases, and the agreement between flight and predicted values of $d\Phi/d\beta$ is very good.

Asymmetric-Power Characteristics

The data for the steady sideslips under asymmetric-power conditions are plotted in figures 16 and 17 as a function of sideslip angle. Cross plots for the condition of 10° sideslip toward the live engine are given in figure 18.

With regard to the control characteristics under asymmetric-power conditions, the same general conclusions can

be drawn from both the wind-tunnel and flight data. For each case, figures 16 and 17 indicate that the rudder and aileron are sufficiently powerful for zero-yaw flight at low speeds, although zero-yaw runs were not made in flight due to excessive rudder control forces. Neither the predicted nor flight values of aileron control force are too large, but the rudder control forces (especially the flight values) are excessive.

For the left-engine-throttled condition (fig. 16), the flight and wind-tunnel values of rudder angle are in very good agreement. For the right-engine-throttled tests (fig. 17), however, greater (more left) rudder deflections were needed in flight than were predicted. Comparison of the wind-tunnel data for the left- and right-engine-throttled conditions shows that, as is usually the case, considerably larger rudder deflections are required for the left-engine-throttled condition (right-hand propeller rotation). The flight data of figure 18 show only slightly greater deflections with left engine throttled, and extrapolation of the data of figures 16 and 17 indicates that the magnitude of rudder angle required for zero sideslip would be about the same for either engine throttled.

The correlation between flight and wind-tunnel values of rudder control force is similar to that for the rudder angles. For the left-engine-throttled condition (fig. 16) the agreement is good. Rudder control forces for zero sideslip would be excessive, rudder-free flight appears impossible, and the speed for flight at 10° sideslip with a right control force of 180 pounds is 154 miles per hour. For the right-engine-throttled condition (fig. 17), the wind-tunnel data show that, with a rudder control force of 180 pounds, steady flight could be maintained at nearly zero sideslip at the test speeds; whereas in flight the forces were too large to permit zero sideslip flight and a left sideslip of about 10° accompanied a 180-pound control force at 142 miles per hour. Most of the difference in rudder control-force values between the flight and wind-tunnel tests can be ascribed to the corresponding differences in rudder deflection.

The correlation in the values of aileron angle and angle of bank is considered good, especially for the right-engine-throttled condition. The computed aileron control forces, based on estimated hinge moments, are larger than those for flight, but indicate the same general characteristics.

Aileron Rolls

The variation of the maximum rolling velocity at sea level and change in aileron control force with total aileron angle in rudder-fixed aileron rolls for the climb and landing conditions are presented in figures 19 and 20. In all cases it is seen that the agreement between flight and wind-tunnel results is excellent. The change in sideslip angle between the start of the maneuver and the time of maximum rolling velocity is shown in figure 19 for one airspeed, and for the example shown the change is in a favorable direction. The agreement between flight and wind-tunnel results is indicative of satisfactory prediction of the yawing characteristics, which are important in estimating the rolling velocities. The usual method of predicting maximum rolling velocities includes a reduction factor to account for the usually unfavorable yaw due to aileron deflection and would not have given as accurate predictions as the method of reference 8 in which the yawing characteristics are estimated in more detail.

A summary cross plot derived from the data of figure 19 is given in figure 21 in which the change in total aileron angle and maximum $pb/2V$ corresponding to an 80-pound control force are plotted as a function of airspeed. Both the flight and wind-tunnel data indicate that, although the aileron effectiveness is satisfactory, $pb/2V$ at high speed is seriously limited by the high control forces.

CONCLUSIONS

Based on the data presented in this report, the following conclusions can be drawn with regard to the correlation of the lateral- and directional-stability and -control characteristics of a low-wing, twin-engine patrol airplane as predicted from wind-tunnel tests and as measured in flight:

1. Wind-tunnel predictions indicated the critical unsatisfactory directional and lateral characteristics. The most serious of these were the generally high rudder control forces, which resulted in unsatisfactory asymmetric-power control, and high aileron control forces, which seriously limited the rolling ability at normal and high speeds.

2. The wind-tunnel data were, in general, sufficiently accurate to indicate the chief reasons for the unsatisfactory characteristics and possible methods of improvement.

Ames Aeronautical Laboratory,
National Advisory Committee for Aeronautics.
Moffett Field, Calif.

REFERENCES

1. Stevens Jr., Victor I., and McCullough, George B.: Flying Qualities of the PV-1 as Estimated from Wind-Tunnel Tests. NACA CMR, Sept. 1943.

2. Delany, Noel K., and Kauffman, William H.: Correlation of Wind-Tunnel Predictions with Flight Tests of a Navy PV-1 Airplane. I.- Longitudinal-Stability and -Control Characteristics. NACA RMR No. A5D04, 1945.

3. Anon.: Erection and Maintenance Instructions for Army Model RB-34 Series, British Models Ventura BI, II, IIA, and IV Airplanes. Tech. Order No. 01-55EA-2, Nov. 1943 (revised April 30, 1944).

4. Rogallo, Francis M., and Purser, Paul E.: Wind Tunnel Investigation of a Plain Aileron with Various Trailing-Edge Modifications on a Tapered Wing. I - Aileron with Fixed Inset Tabs. NACA ARR, Sept. 1942.

5. Holtzclaw, Ralph W., and Erickson, Myles D.: Wind-Tunnel Investigation of Flap, Aileron, and Exterior Bomb Installations on a 24-Inch Constant-Chord North American XB-28 Wing Model. NACA ARR, July 1942.

6. Crane, Robert M.: Computation of Hinge-Moment Characteristics of Horizontal Tails from Section Data. NACA CB No. 5B05, 1945.

TABLE I.- WING AND VERTICAL-TAIL DIMENSIONS OF THE AIRPLANE

Item	Wing	Vertical tail (total)
Area, sq ft	[a]576	64.11
Span, ft	65.5	7.89
Aspect ratio	[b]7.79	1.95
Taper ratio	[b]3.42:1	----
Dihedral of wing, deg	[c]4°31'	----
Incidence with respect to fuselage reference line, deg	2°	----
Root section	NACA 23018 modified by trailing-edge extension	Approx. NACA 0007
Tip section	NACA 23009	----
Twist (geometric)	None	None
M.A.C., ft	[a]10.27	----
Root chord, ft	[b]13.78	5.20

[a]Includes trailing-edge extension
[b]Exclusive of trailing-extension
[c]Measured on top of main beam

TABLE II.- DIMENSIONS OF MOVABLE SURFACES, OF THE AIRPLANE

Item	Aileron (each)	Rudder (each)	Flap (each)
Area aft of hinge line, sq ft	17.45	[a]15.8	52.3
Span, ft	11.25	7.89	15.72
Percent span	34.35	100	48
Balance type	Boost tab	Paddle balance and boost tab	---
Balance area, sq ft	0	1.6	---
Percent balance	0	10.2	---
Control travel, deg[b]	25.2 up 8.65 down	29.8 left 29.6 right	38
Trim tab area, sq ft	0.64	1.905	---
Tab span, ft	1.936	3.196	---
Tab travel, deg	34.4 up 32.3 down	26.7 left 26.0 right	---
Average boost ratio ($d\delta_t/d\delta$)	0.67	0.22	---

[a]Not including trim tab
[b]Values used during tests

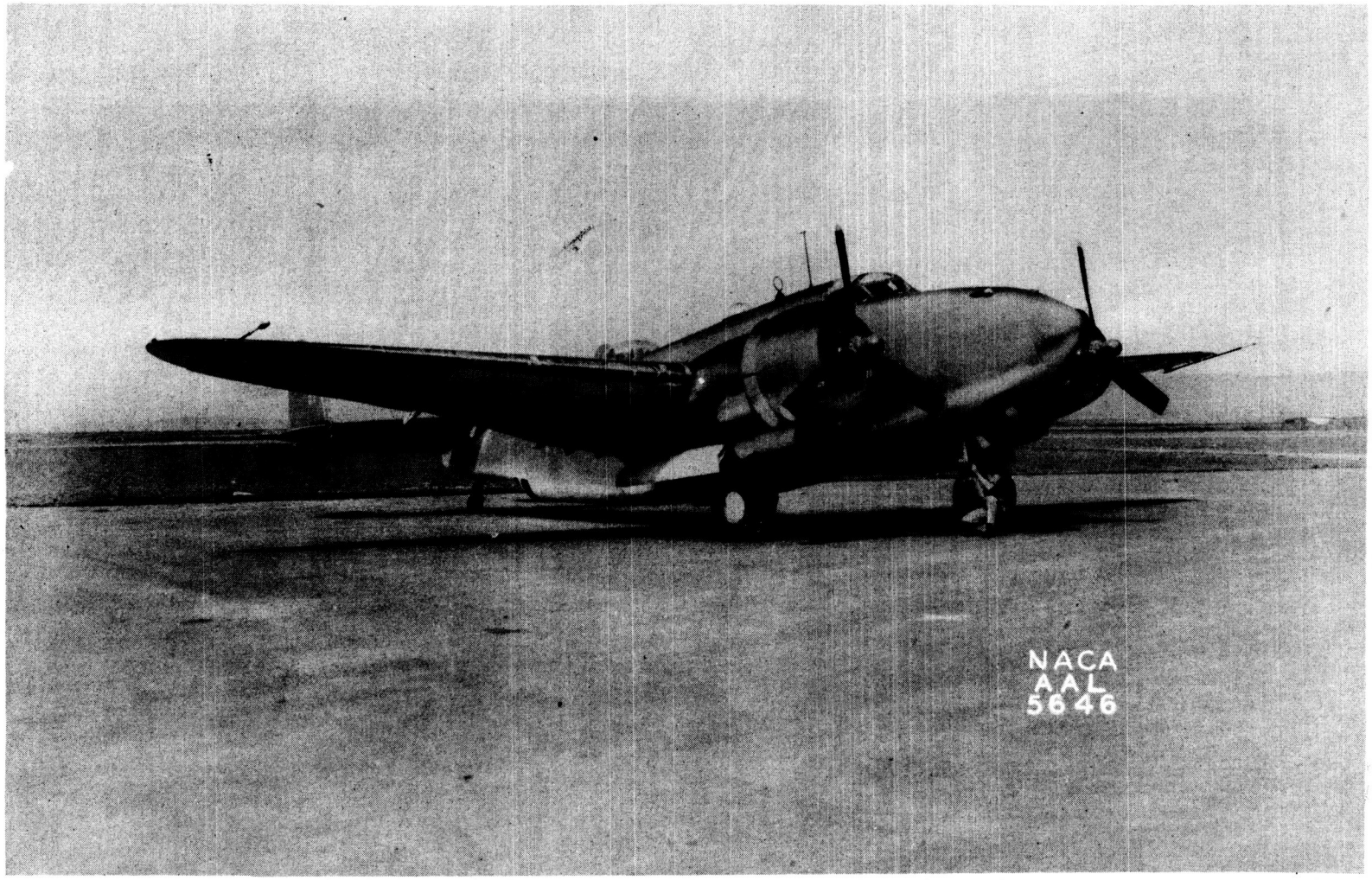

(a) Front view, flaps retracted.

Figure 1.- The airplane as instrumented for flight tests.

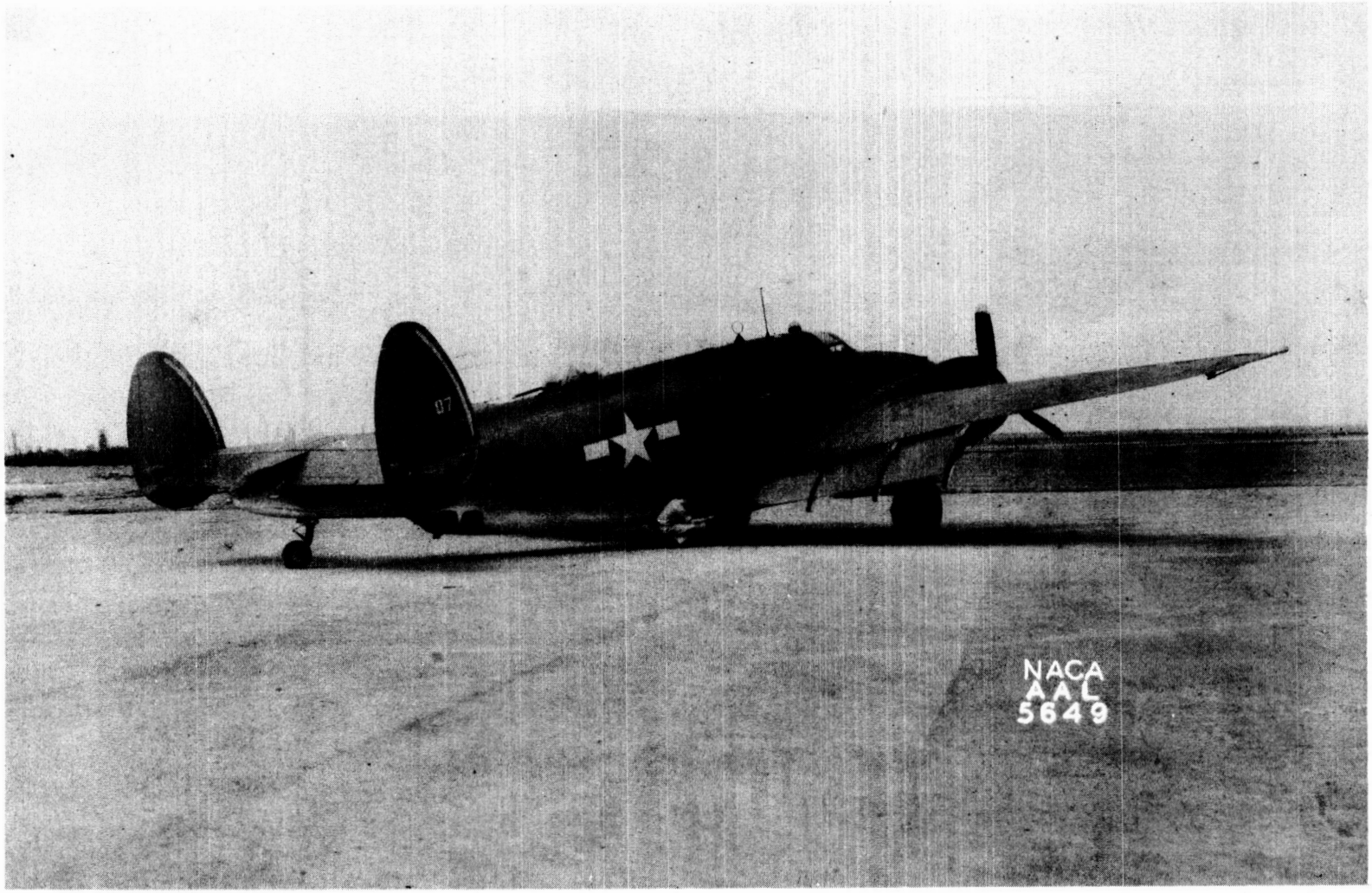

(b) Rear view, flaps deflected.

Figure 1. - Concluded. The airplane as instrumented for flight tests.

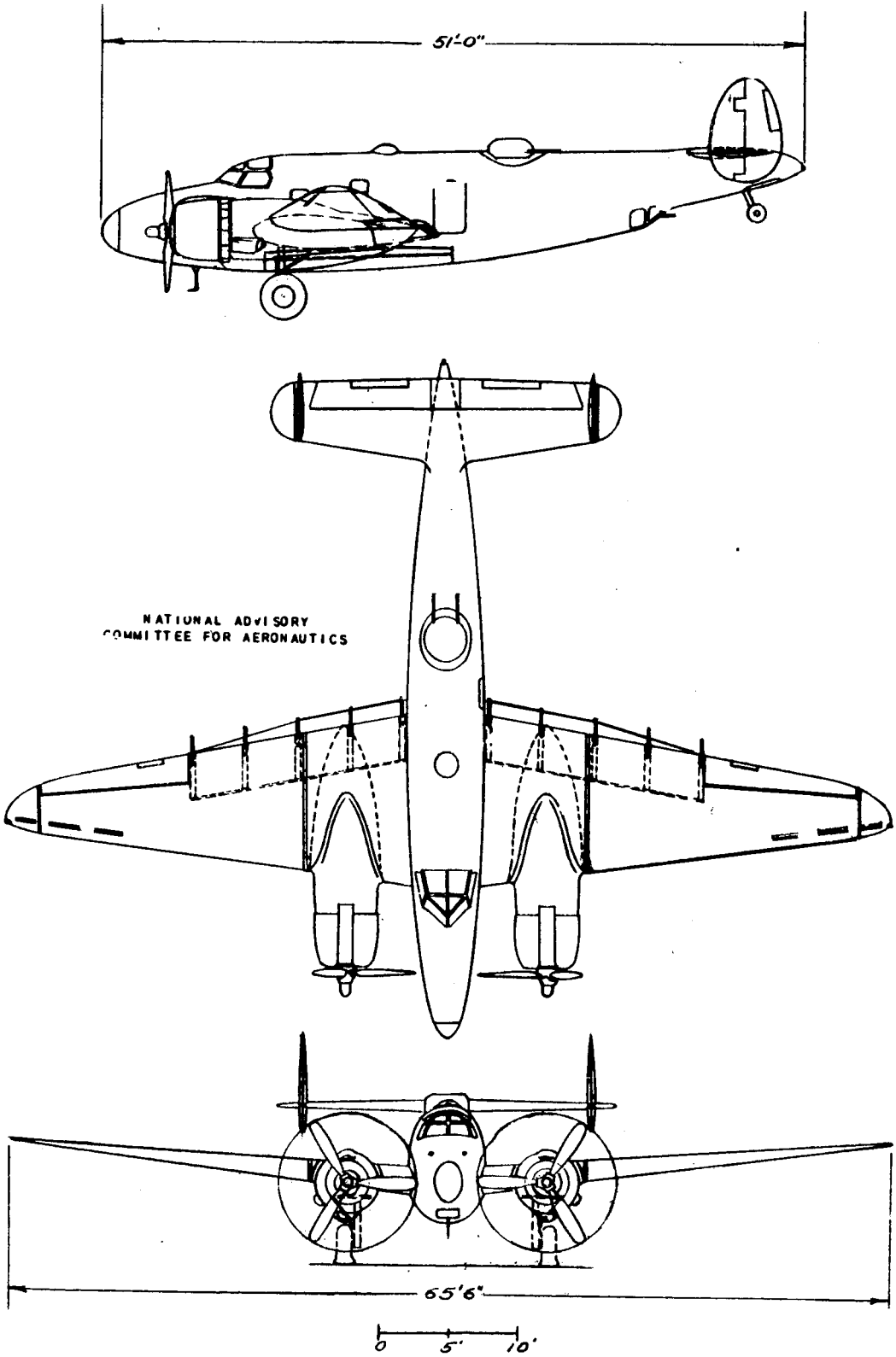

Figure 2.- Three-view drawing of the airplane

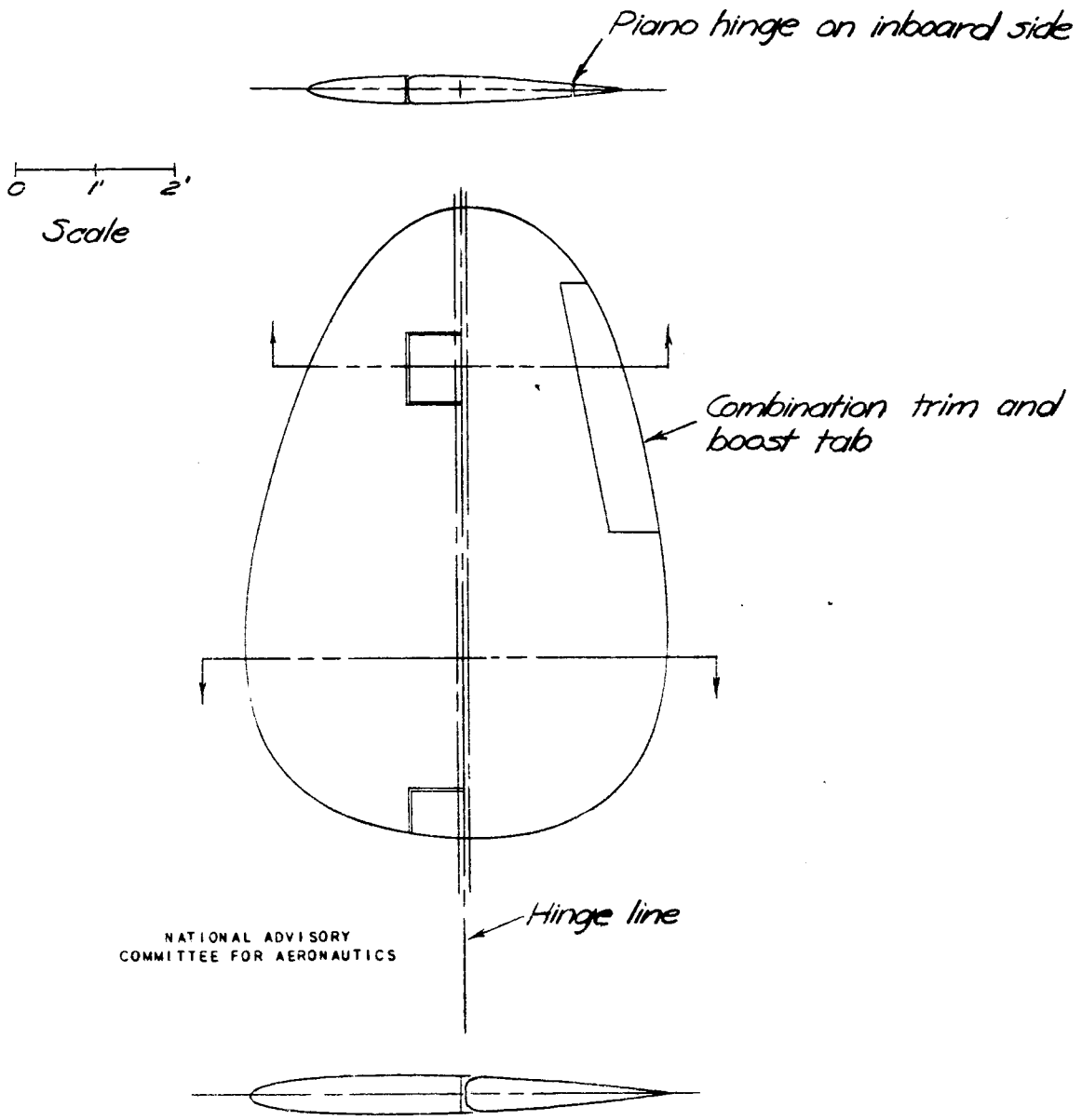

Figure 3. - Sketch of vertical tail surface of the airplane.

A71

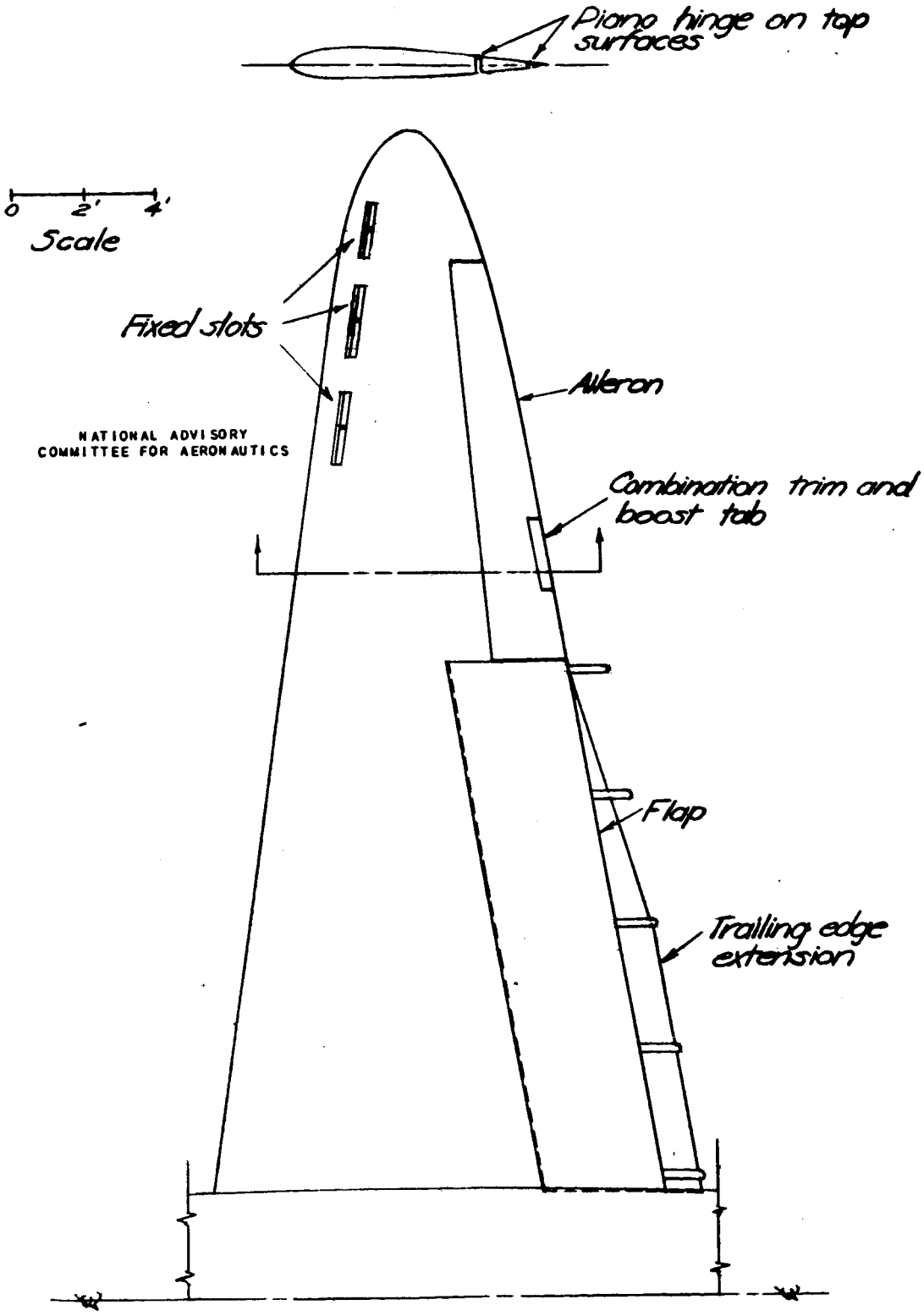

Figure 4.- Sketch of right wing of the airplane

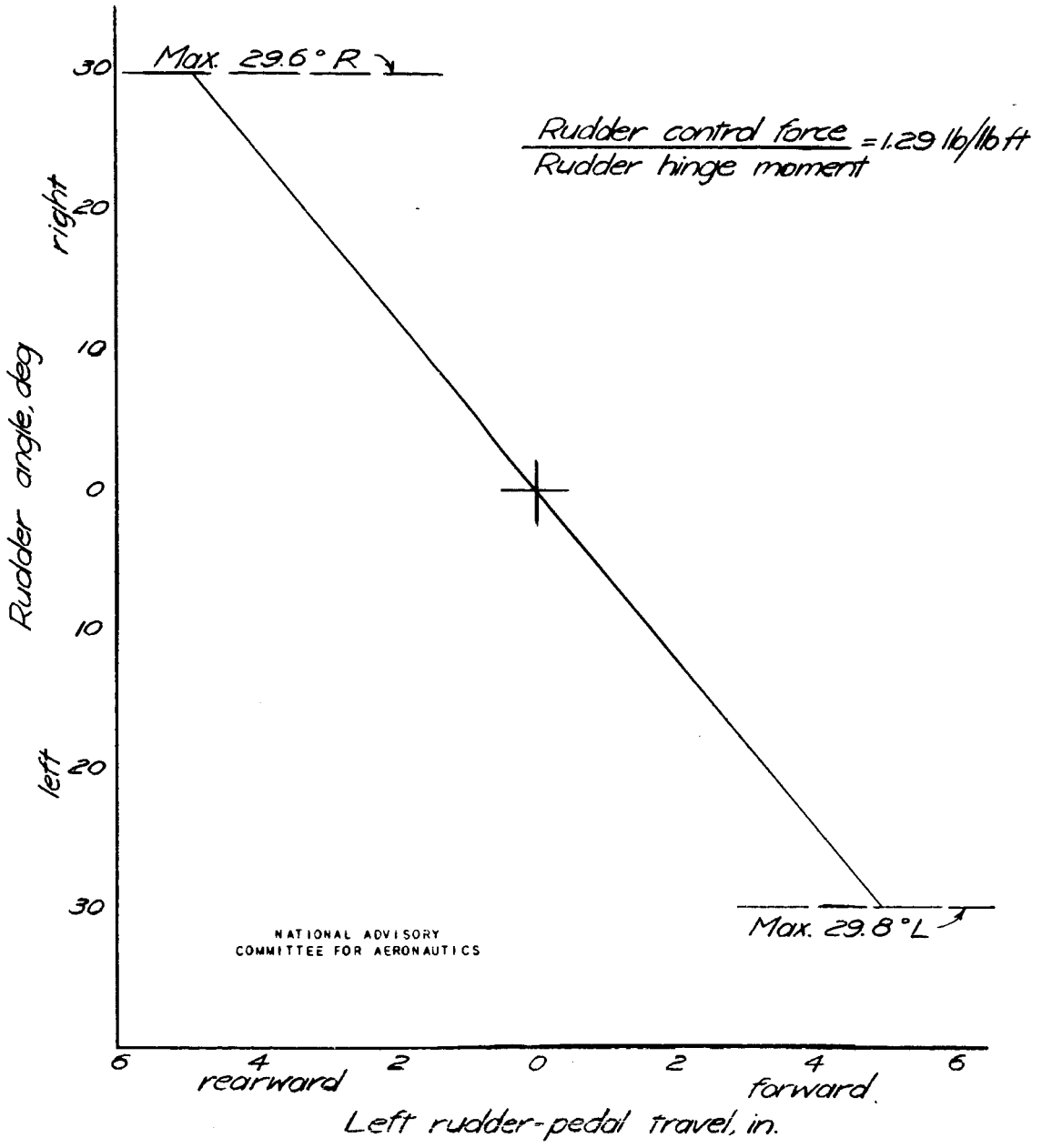

Figure 5.- Variation of rudder angle with rudder-pedal position. Calibrated on the ground with no load on the control surfaces.

A71

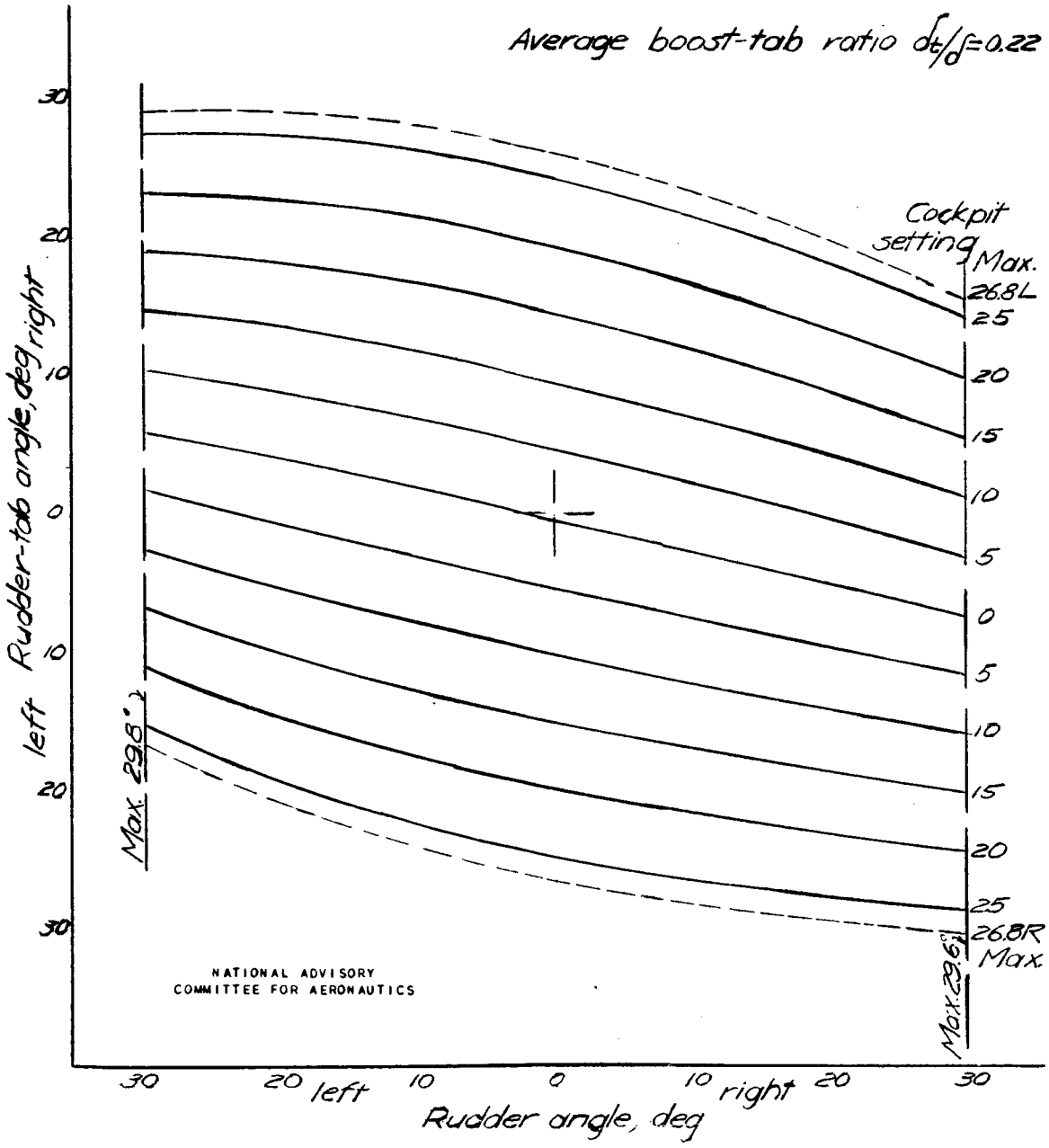

Figure 6. -Variation of rudder-tab angle with rudder angle for different rudder-tab cockpit settings.

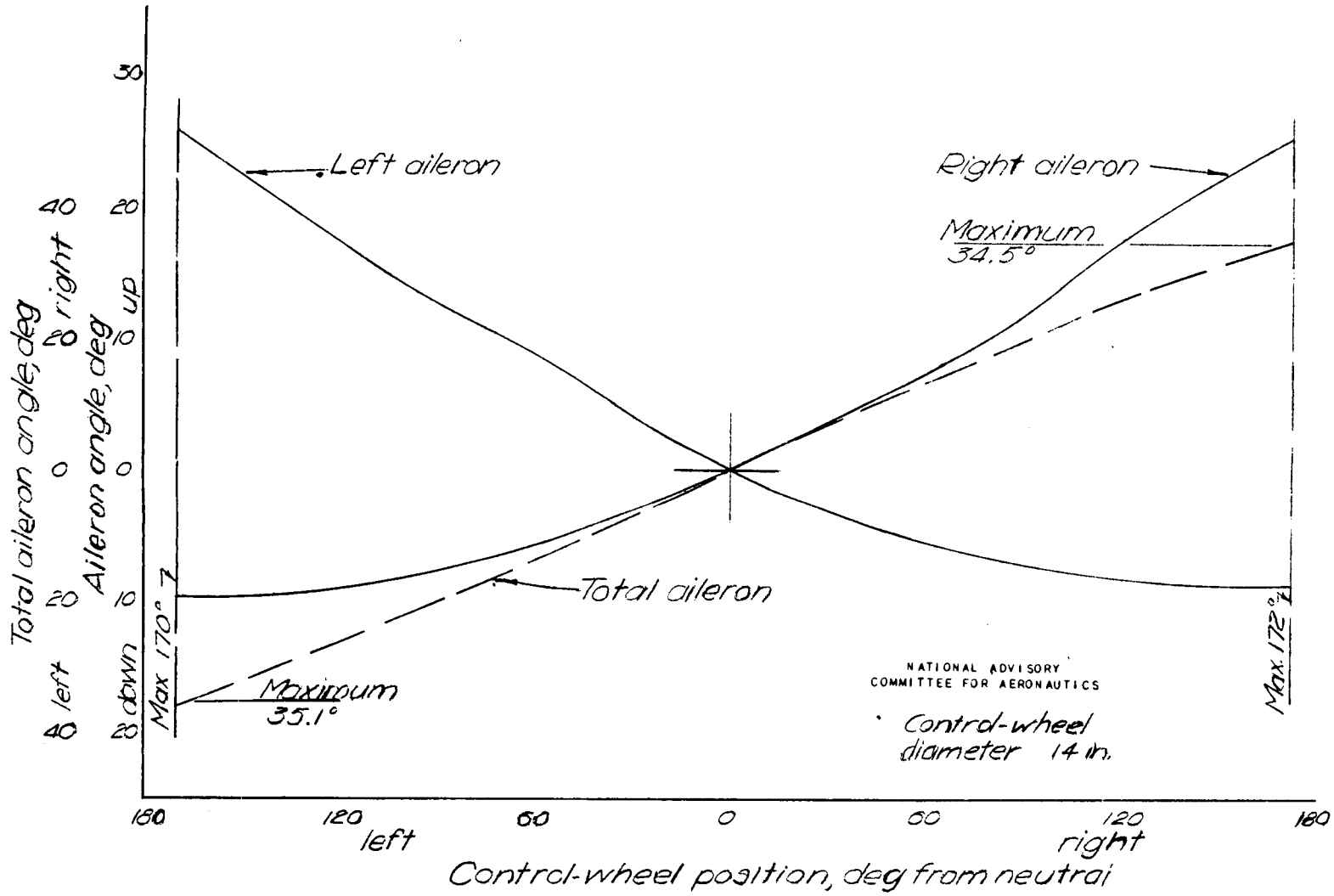

Figure 7.- Variation of aileron angle with control-wheel position. Calibrated on the ground with no load on the control surfaces.

A71

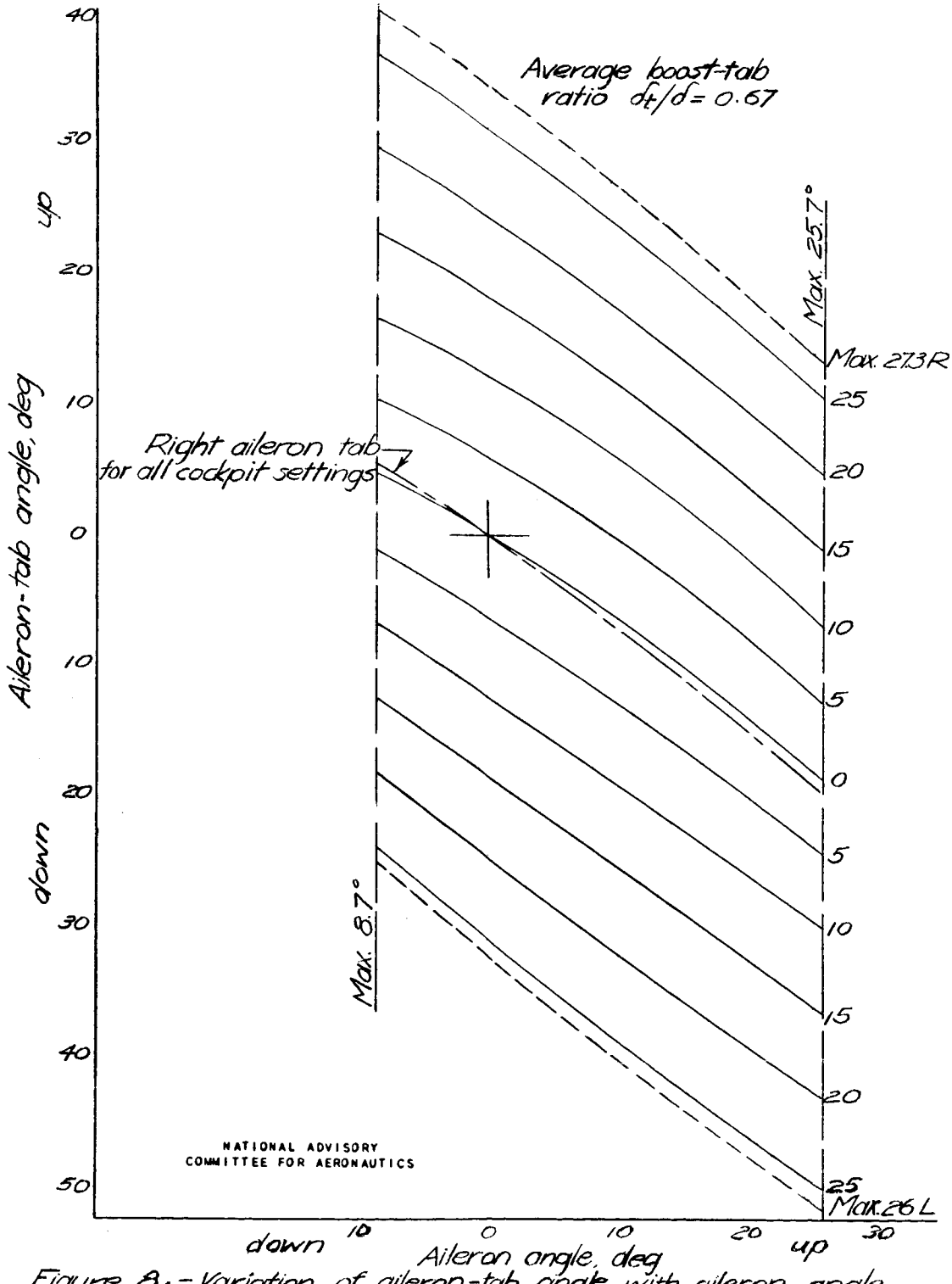

Figure 8.- Variation of aileron-tab angle with aileron angle for different aileron-tab cockpit settings.

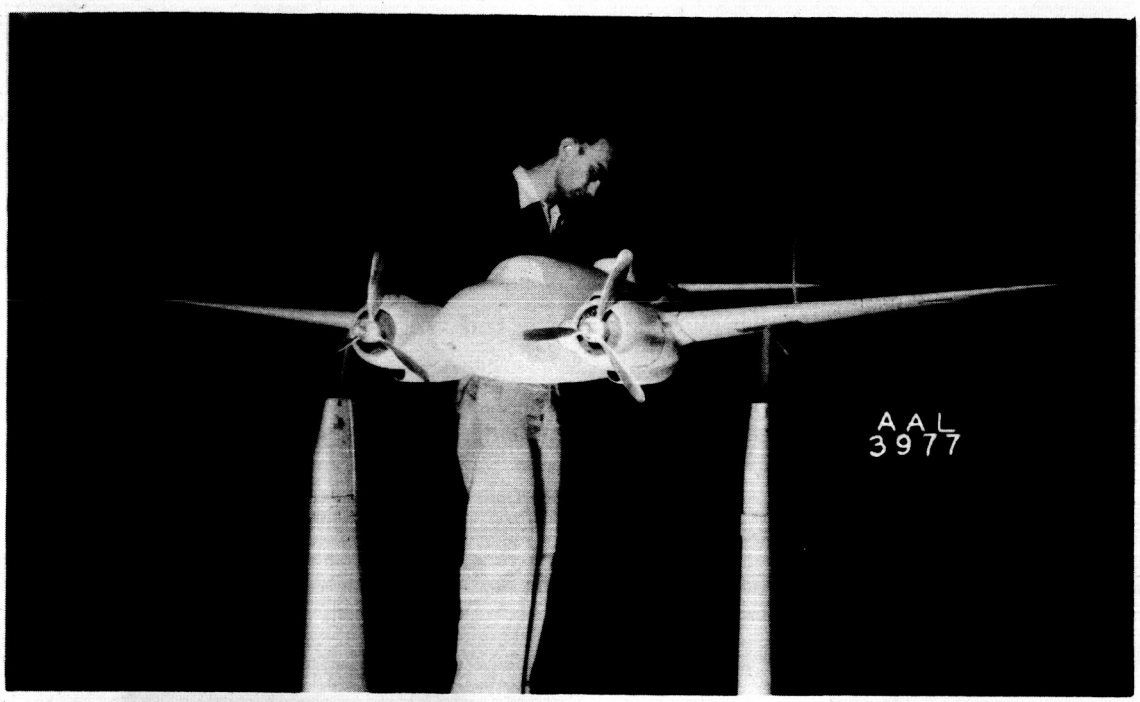

(a) Front view, flaps retracted.

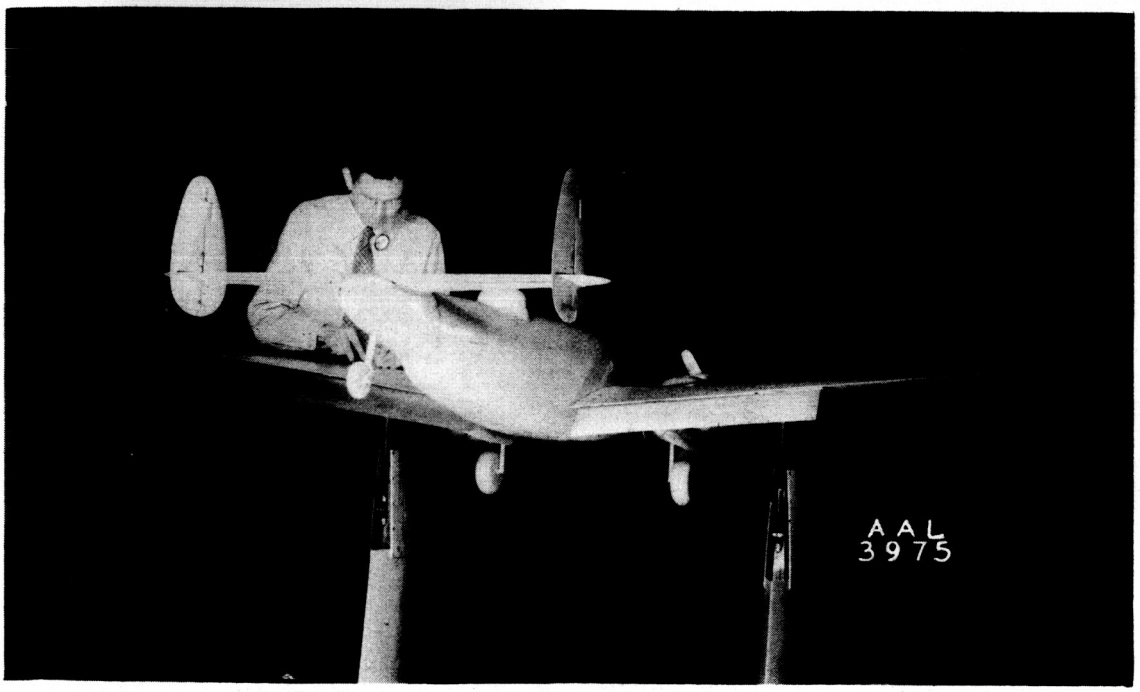

(b) Rear view, flaps down.

Figure 9.- The 1/9-scale model of the airplane mounted in the 7- by 10-foot wind tunnel.

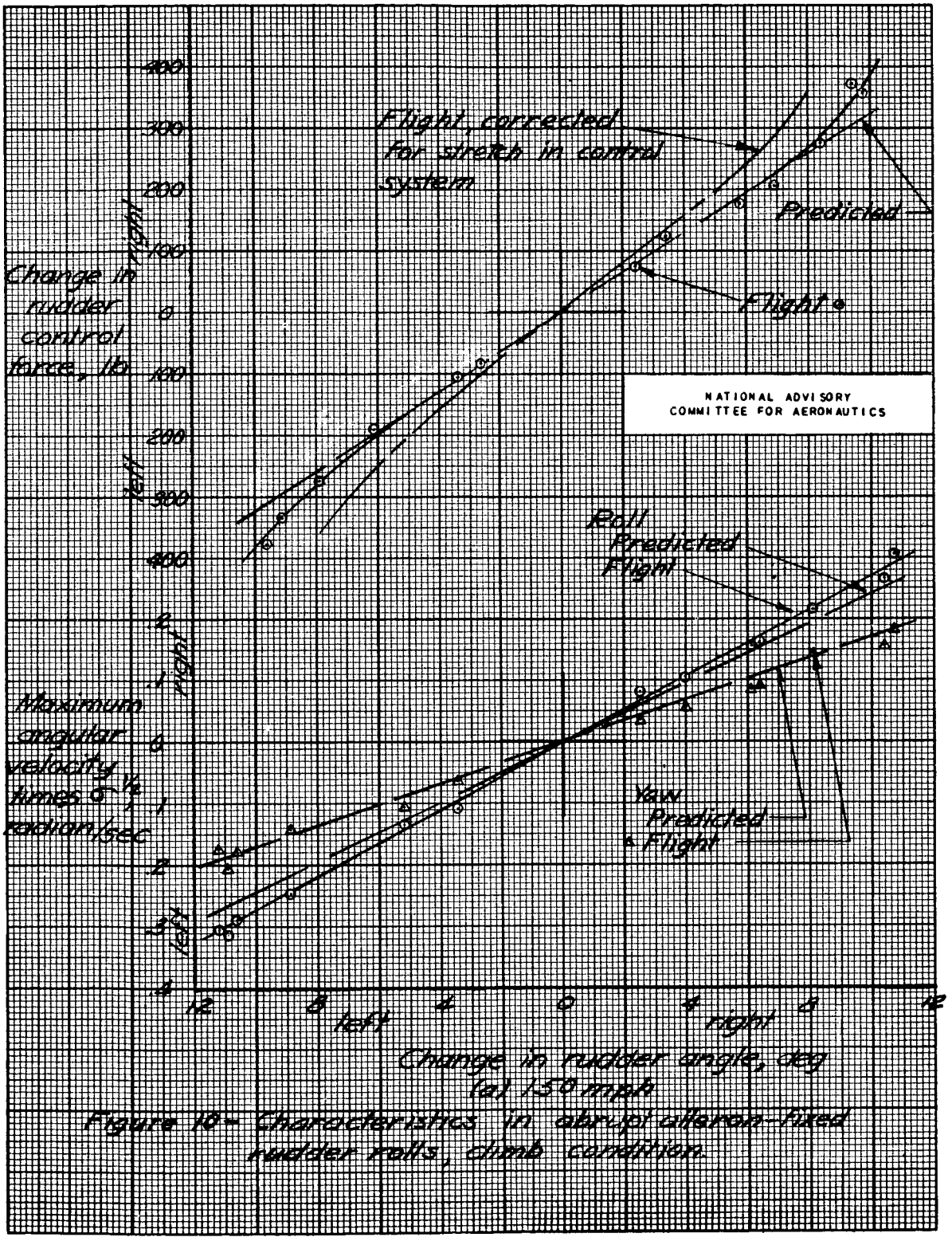

Figure 10.- Characteristics in abrupt aileron-fixed rudder rolls, climb condition.

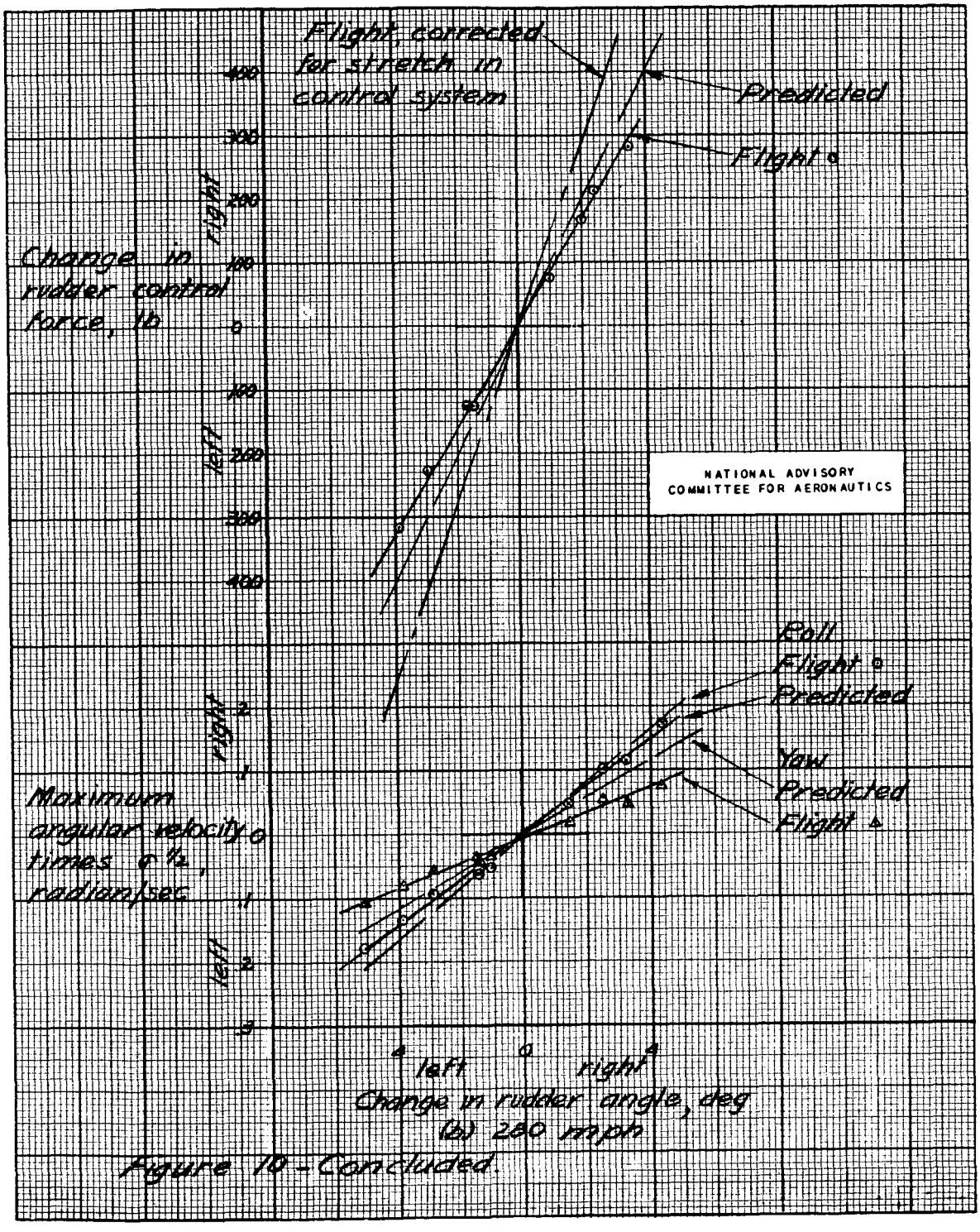

(b) 280 mph

Figure 10 - Concluded.

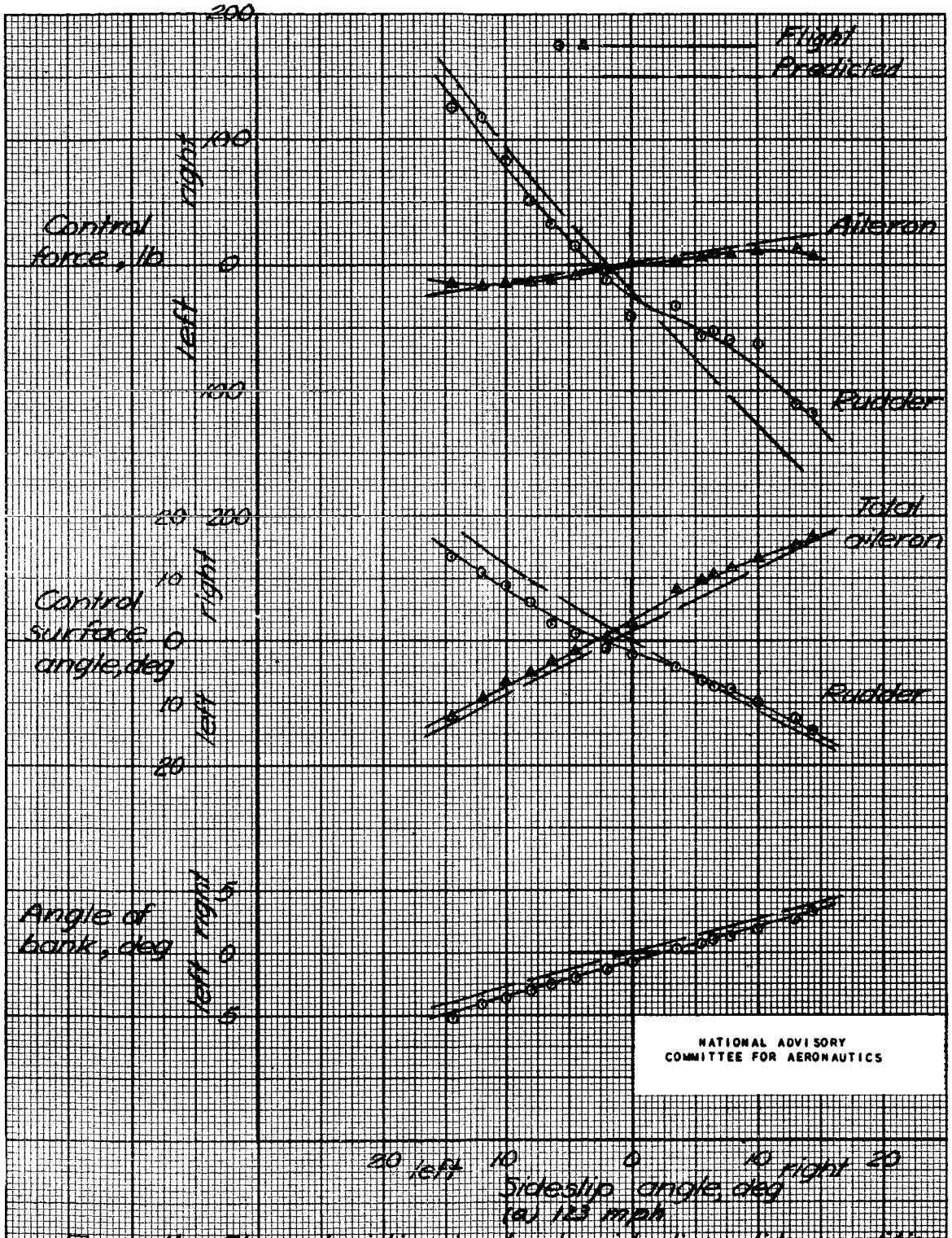

(a) 123 mph

Figure 11 - Characteristics in steady sideslips, glide condition.

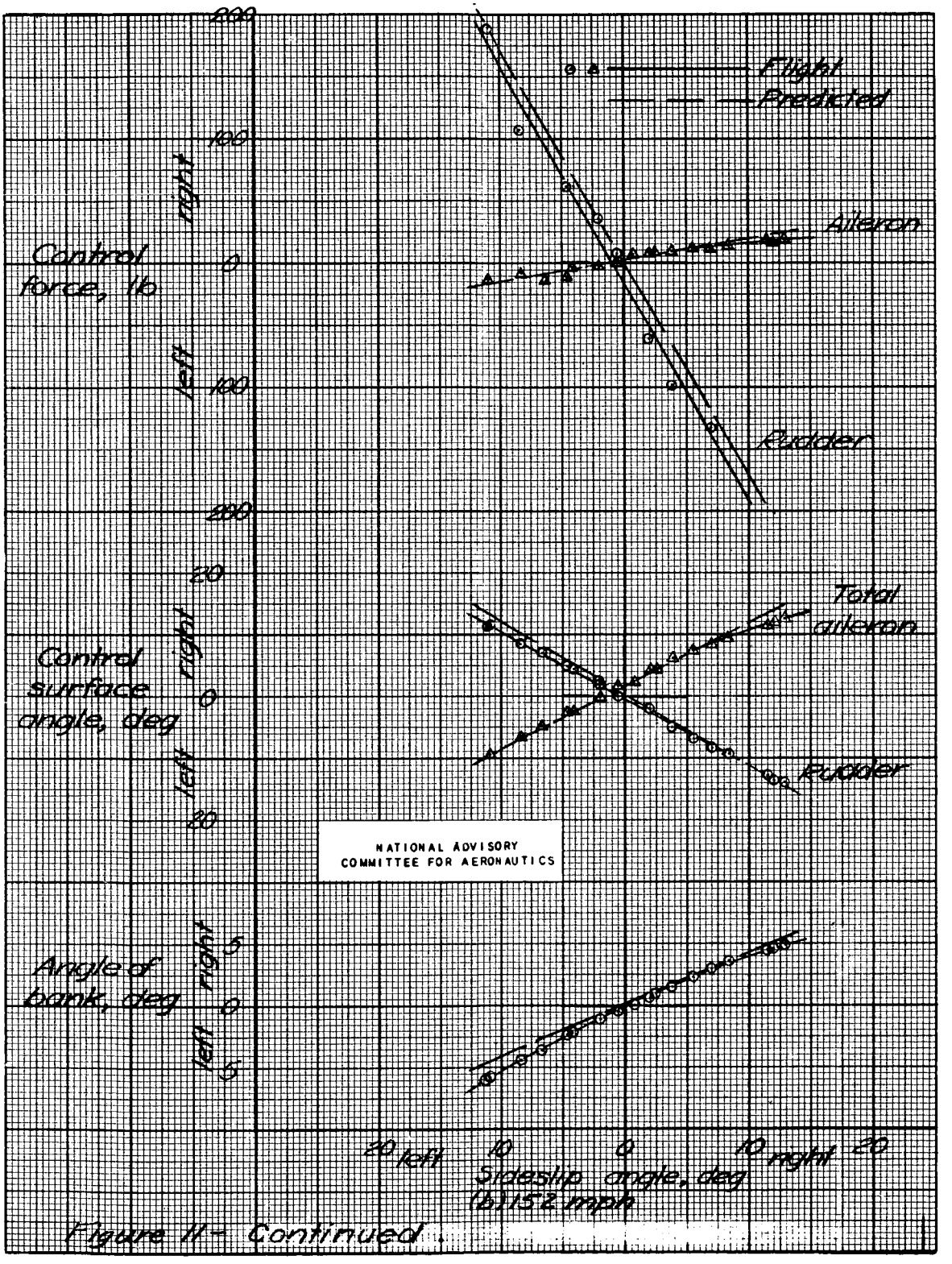

Figure 11 - Continued.

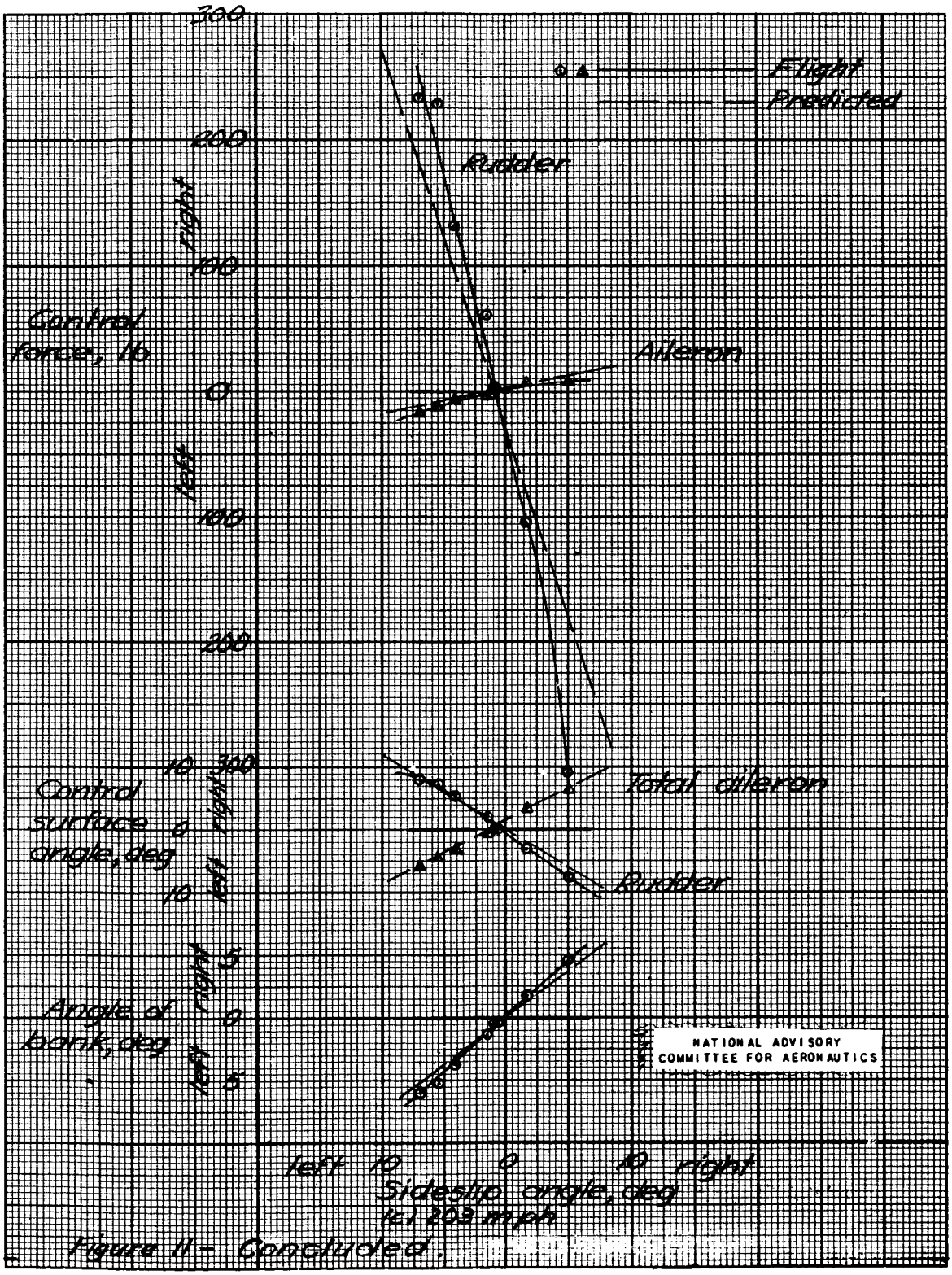

Figure 11 - Concluded.

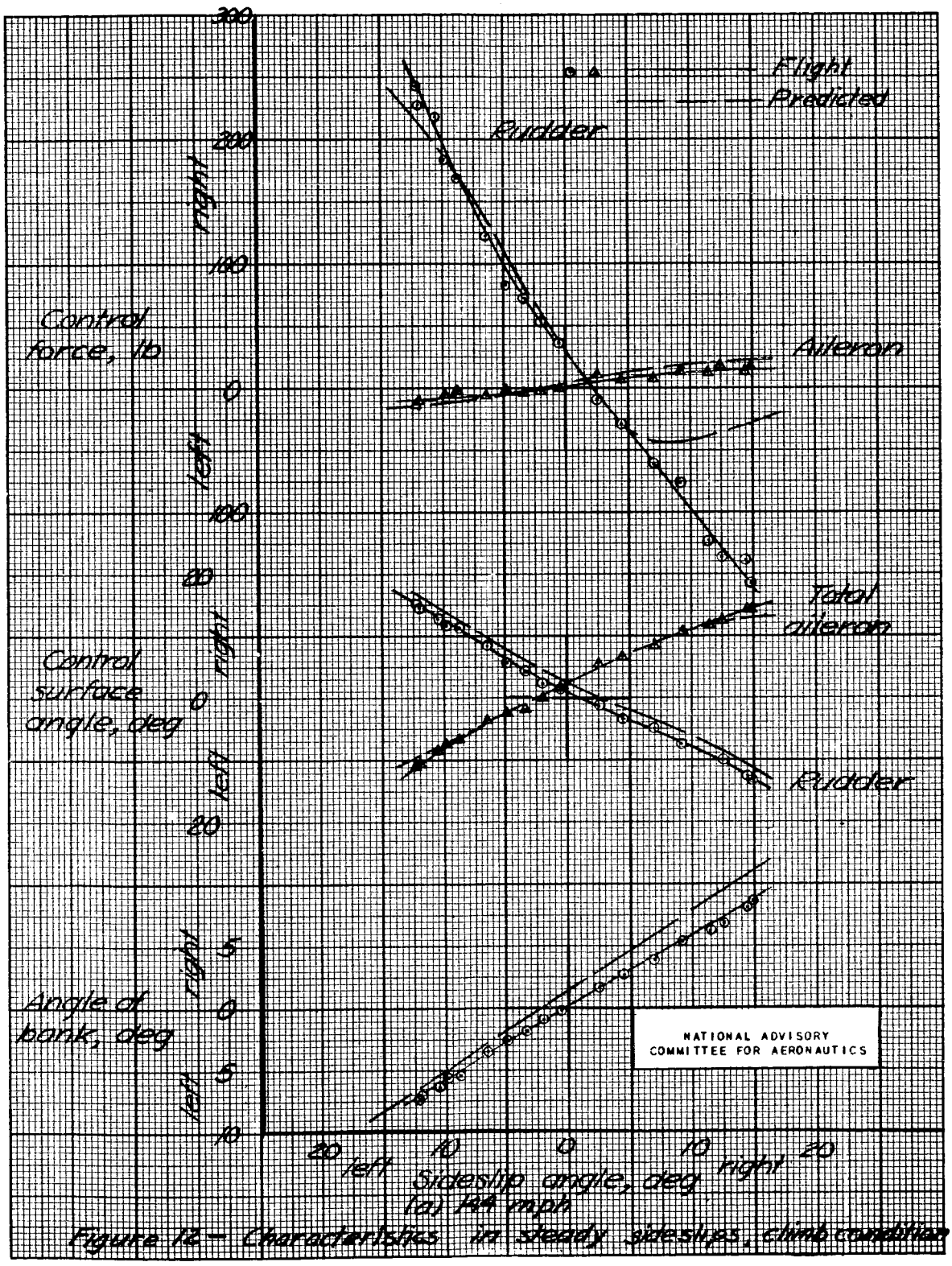

(a) 144 mph

Figure 12 – Characteristics in steady sideslips, climb condition

A71

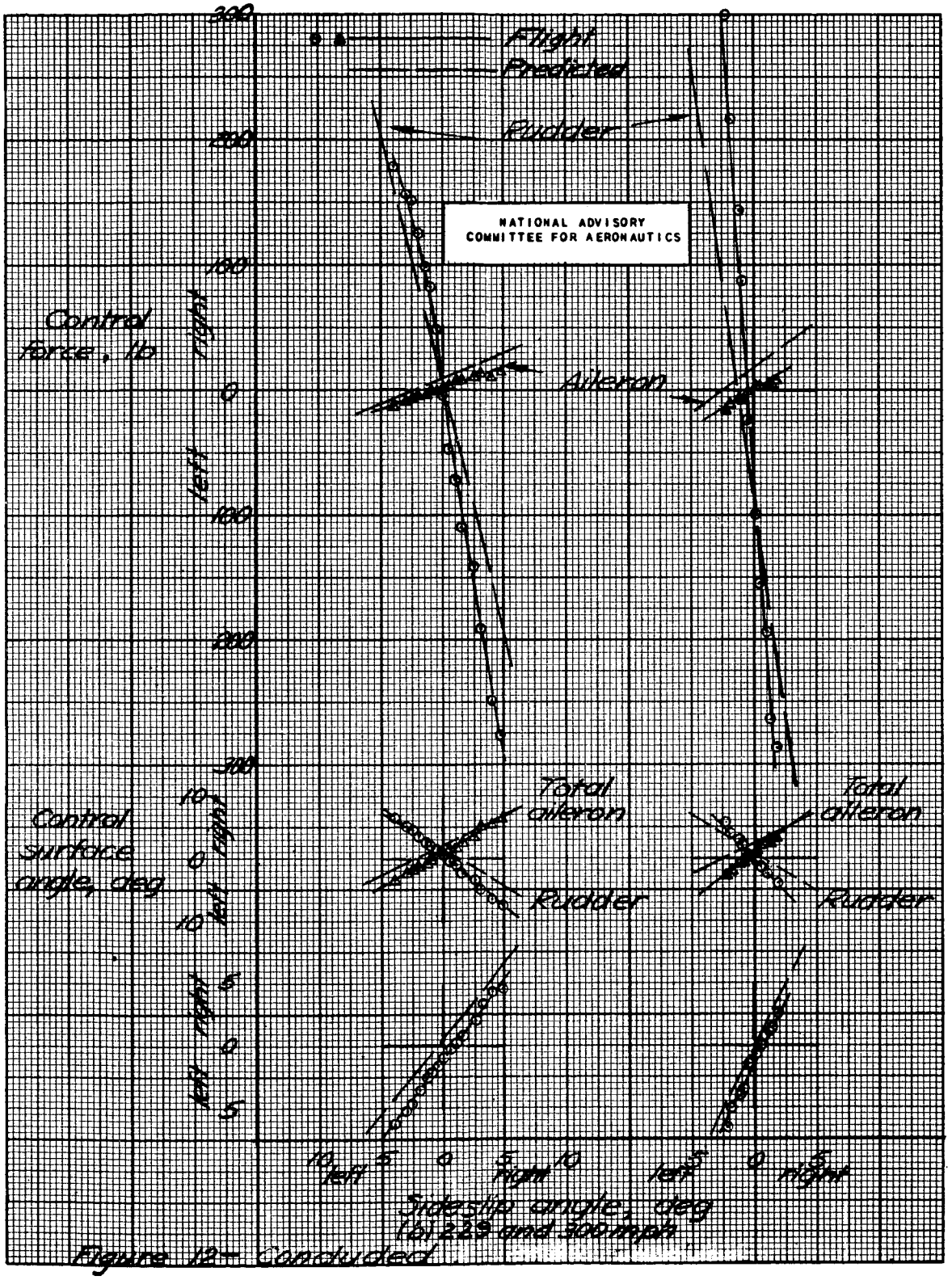

Figure 12.- Concluded

A71

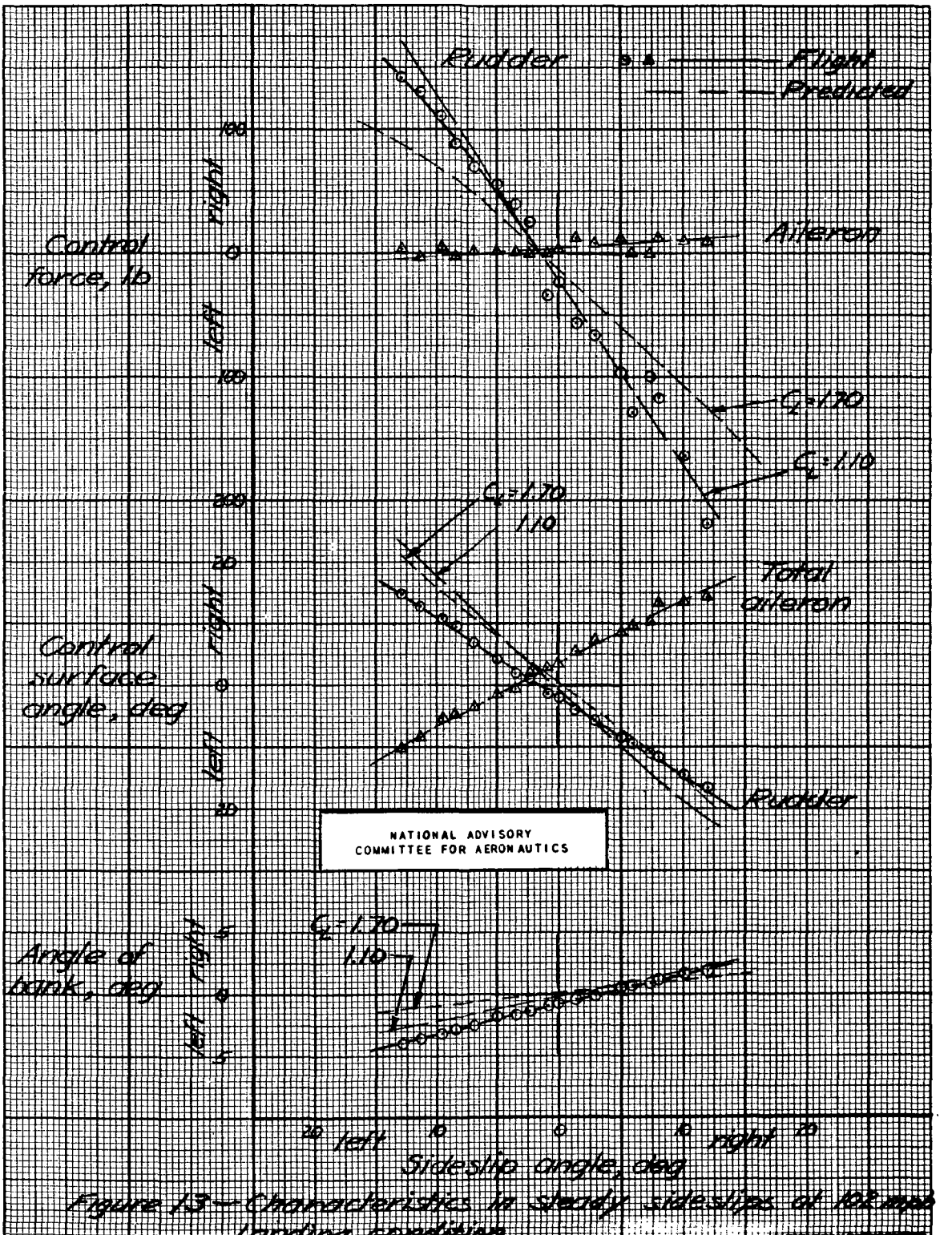

Figure 13.—Characteristics in steady sideslips at 102 mph. Landing condition.

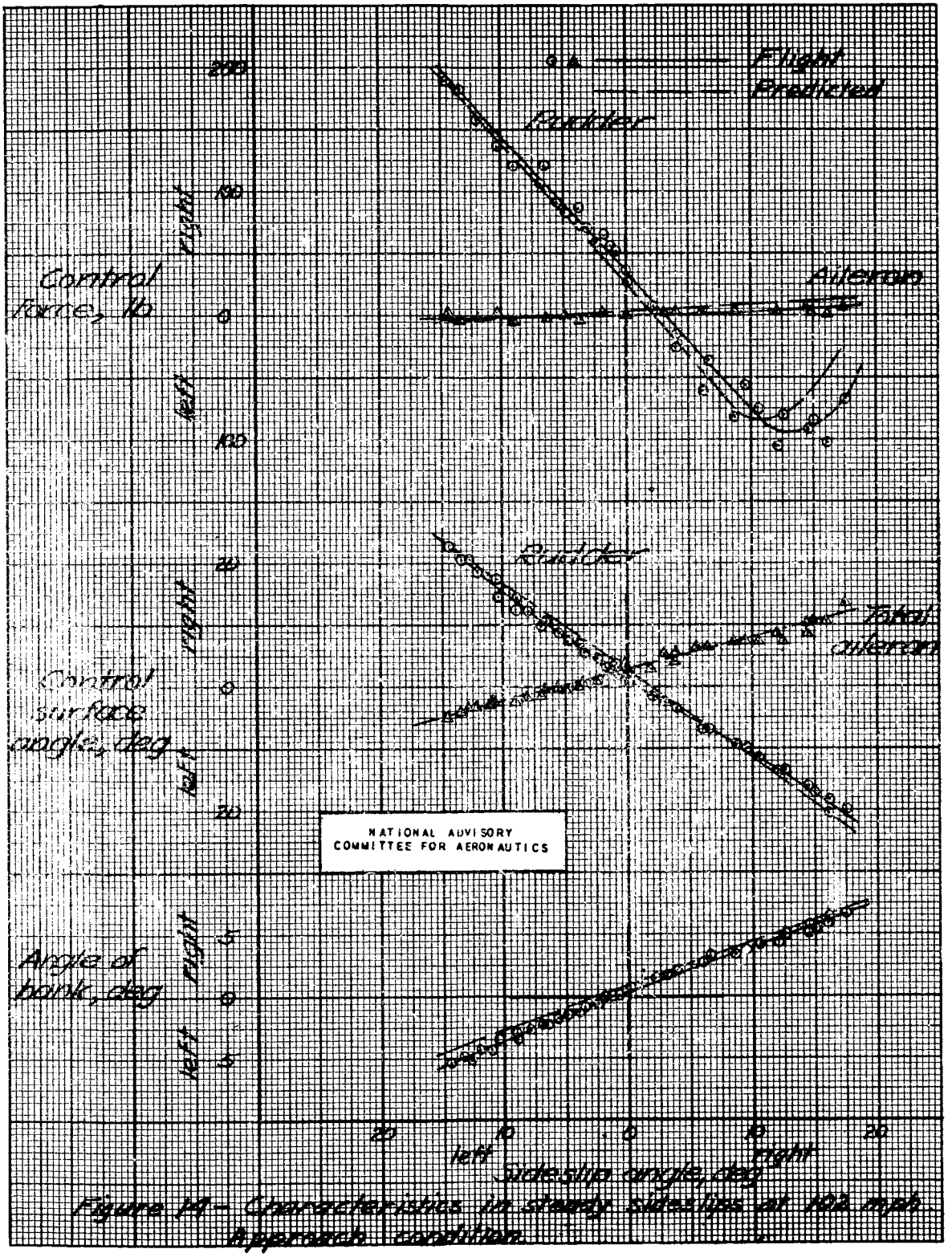

Figure 14.- Characteristics in steady sideslips at 102 mph. Approach condition.

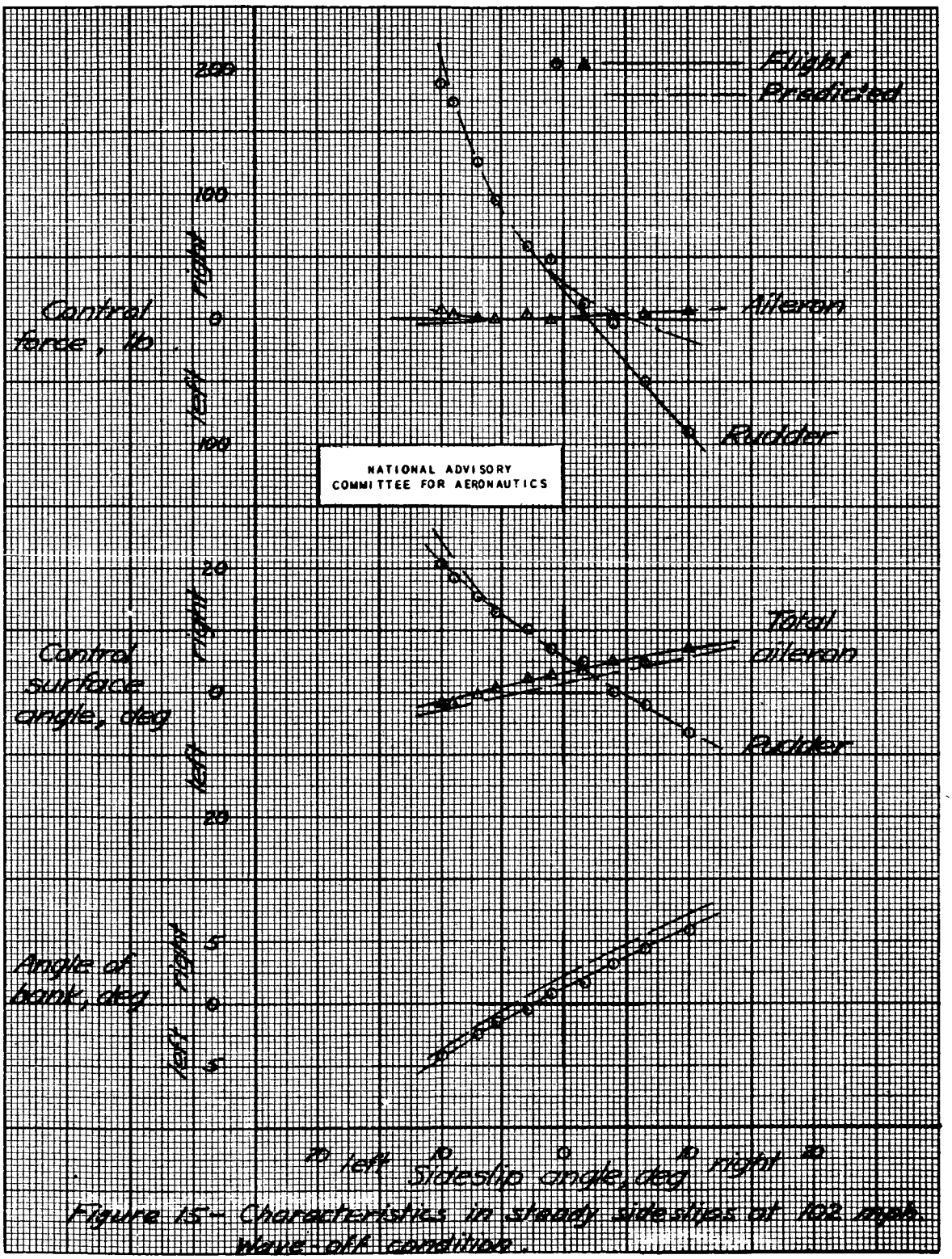

Figure 15.- Characteristics in steady sideslips at 102 mph. Wave-off condition.

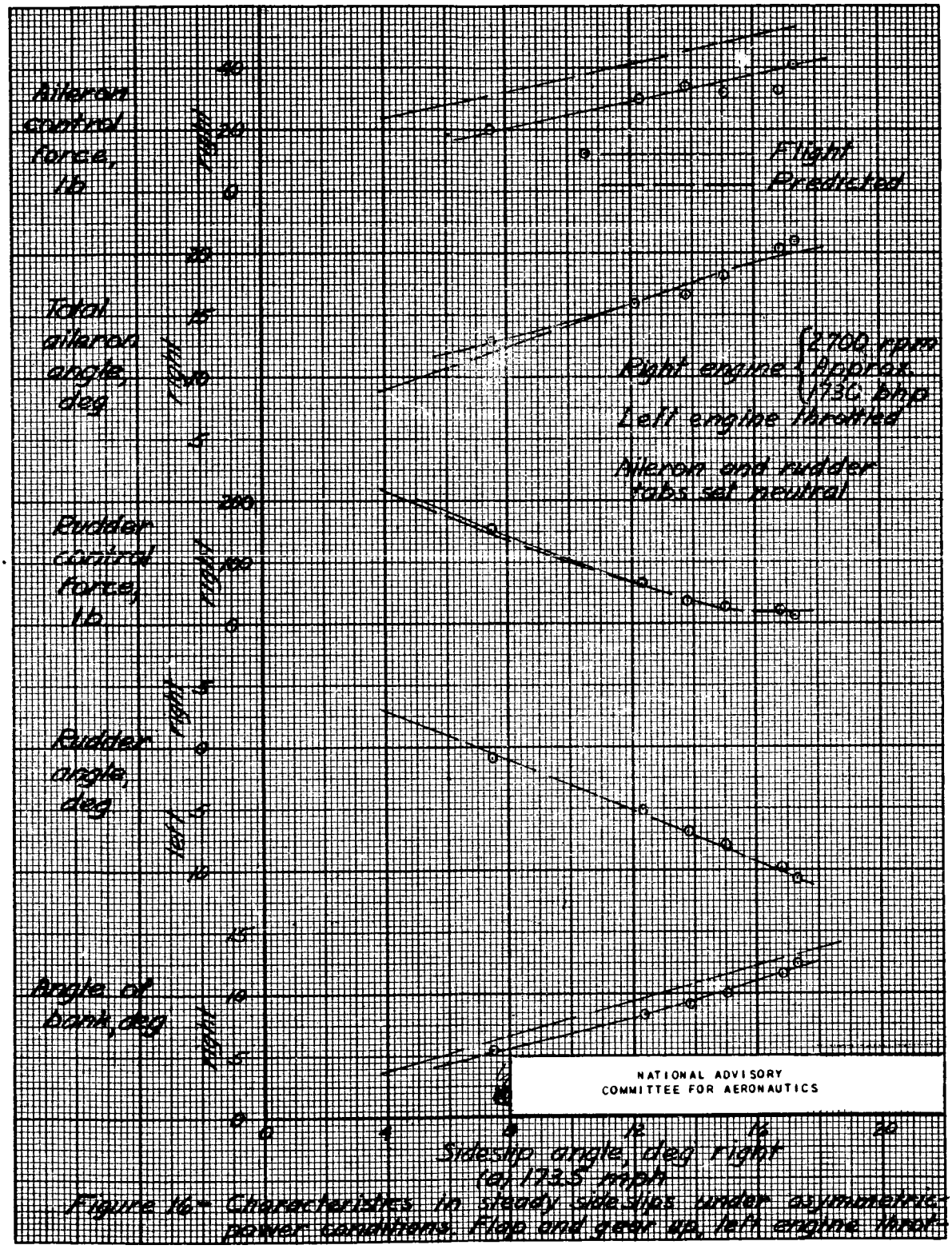

Figure 16.- Characteristics in steady sideslips under asymmetric power conditions. Flap and gear up, left engine throttled

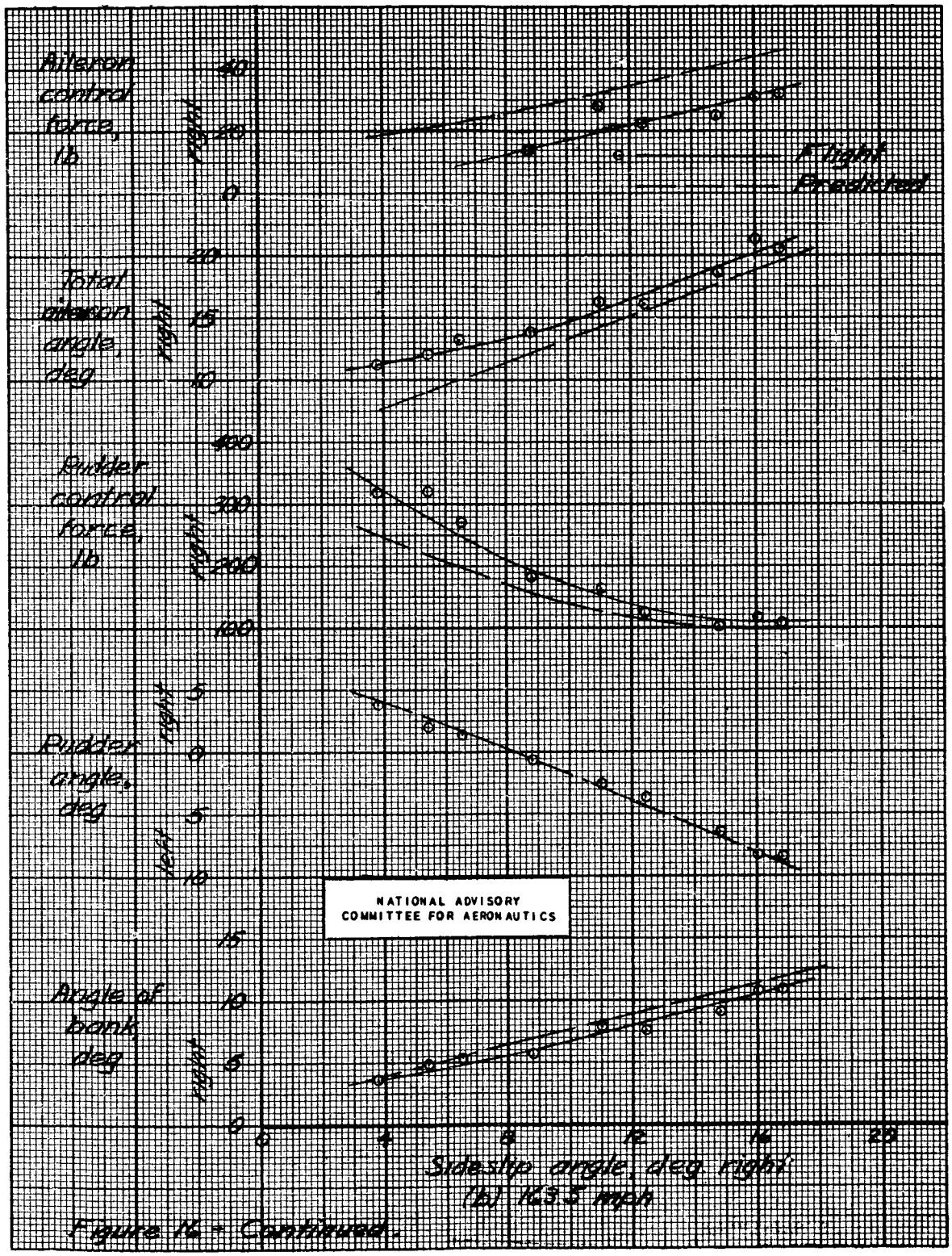

Figure 16 - Continued.

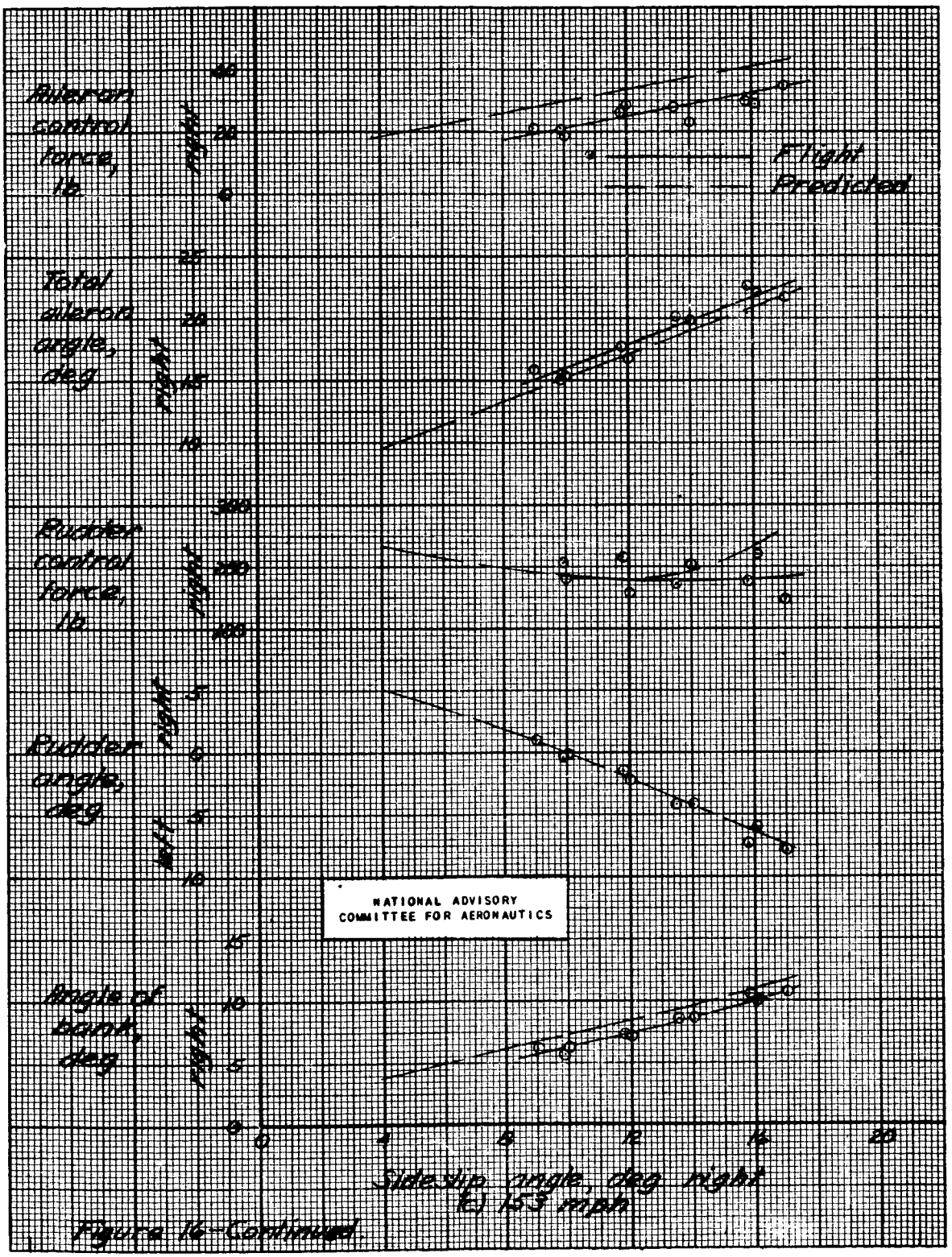

Figure 16—Continued.

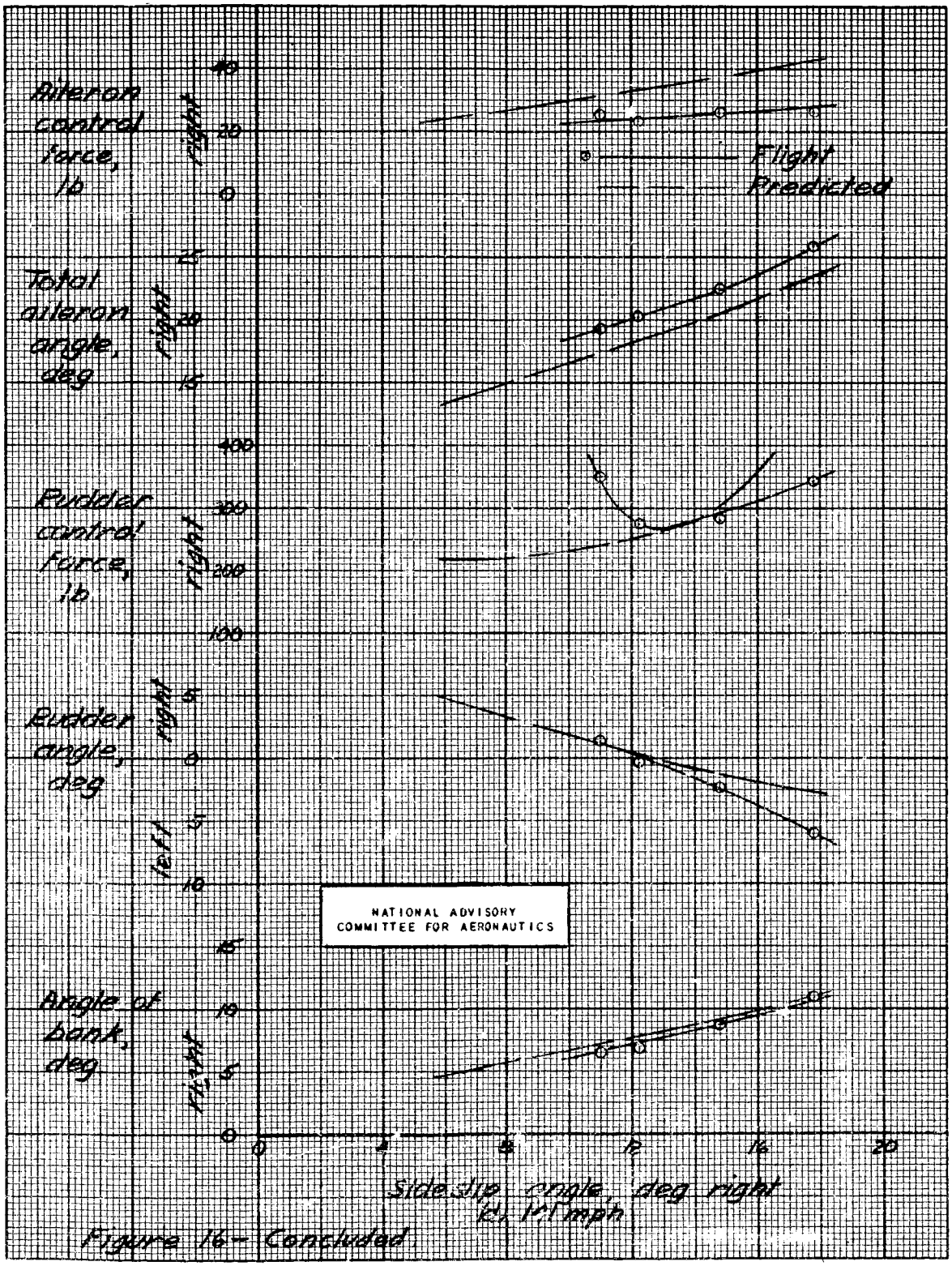

Figure 16- Concluded

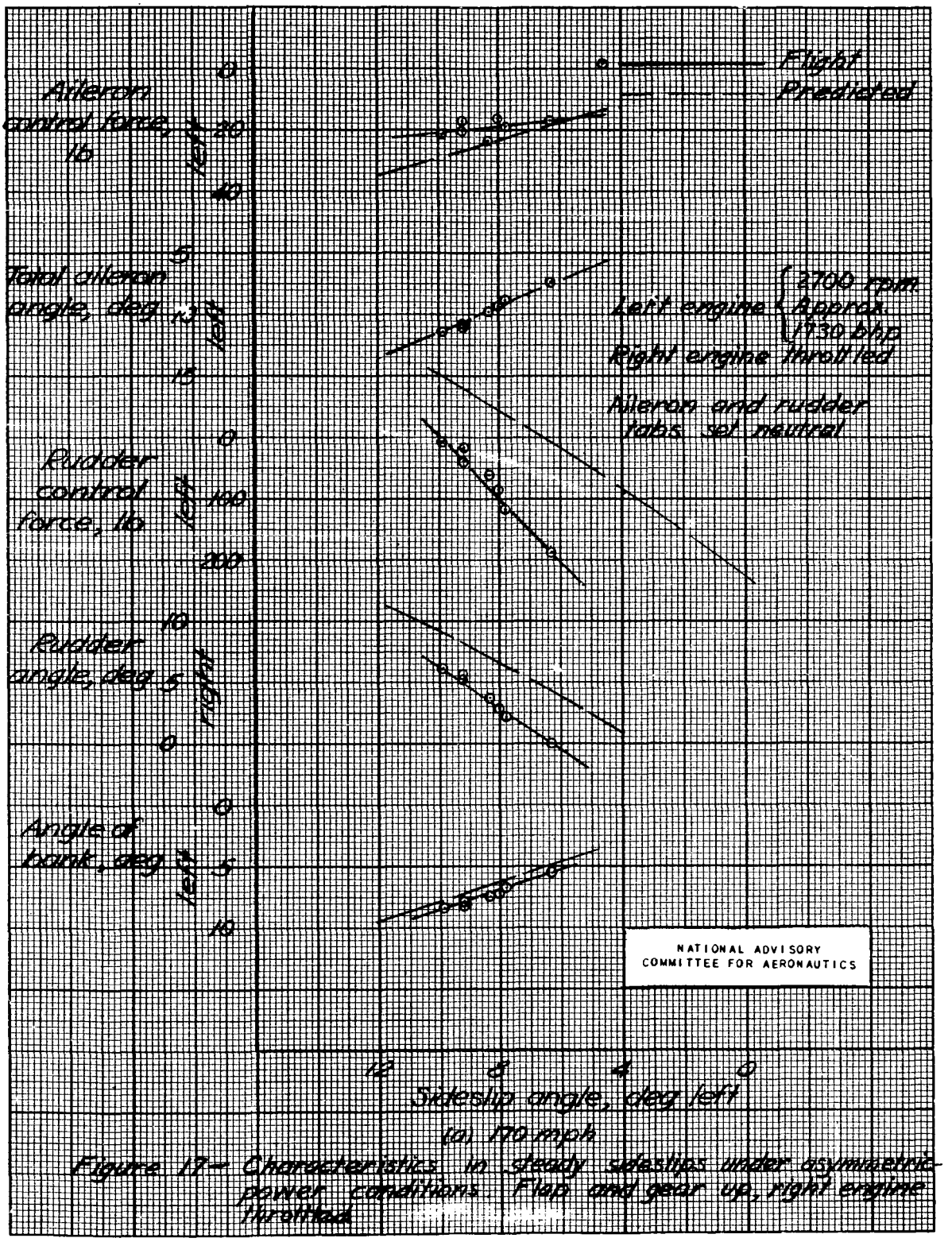

Figure 17.- Characteristics in steady sideslips under asymmetric power conditions. Flap and gear up, right engine throttled.

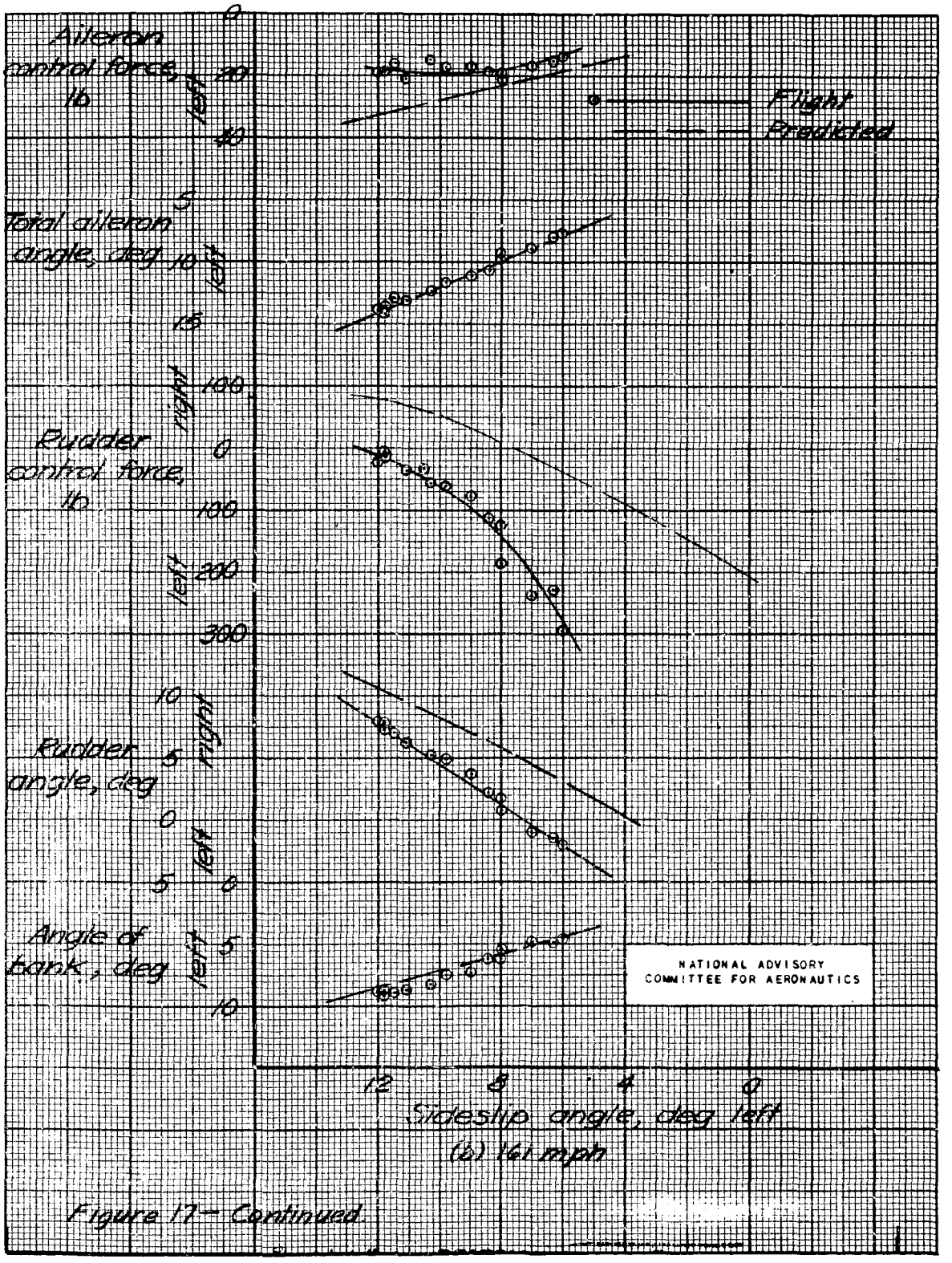

Figure 17— Continued.

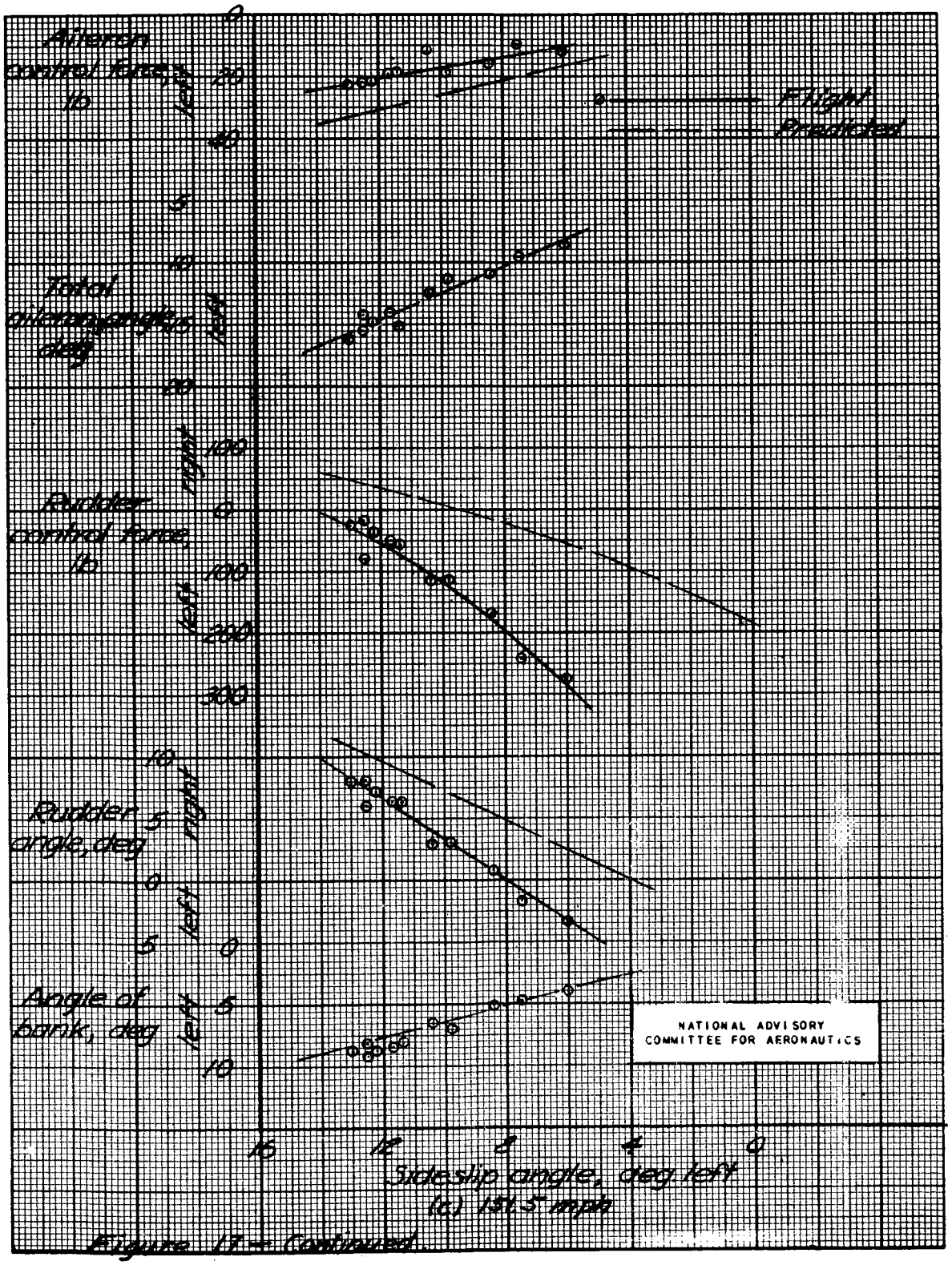

Figure 17.- Continued.

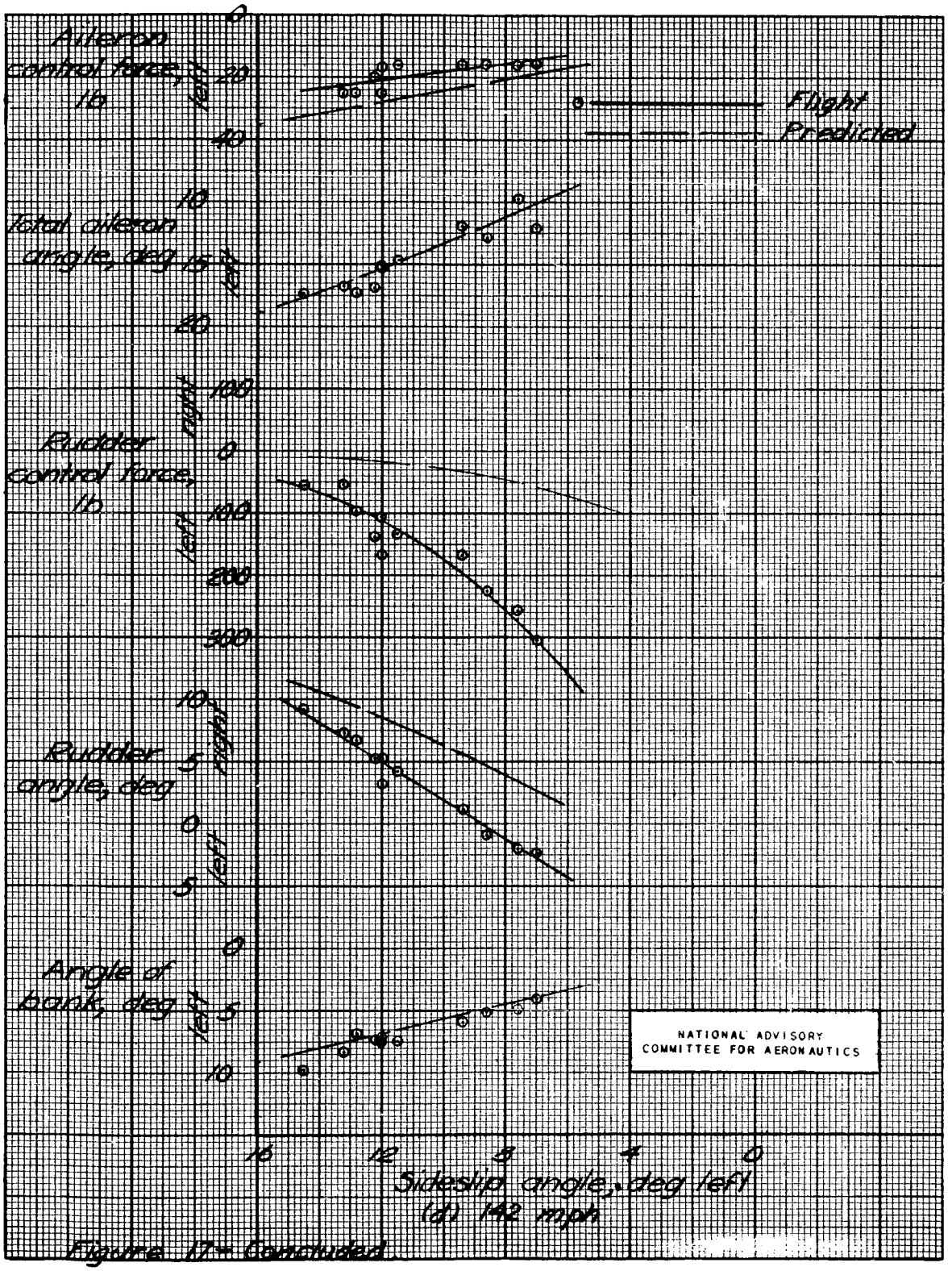

Figure 17.- Concluded.

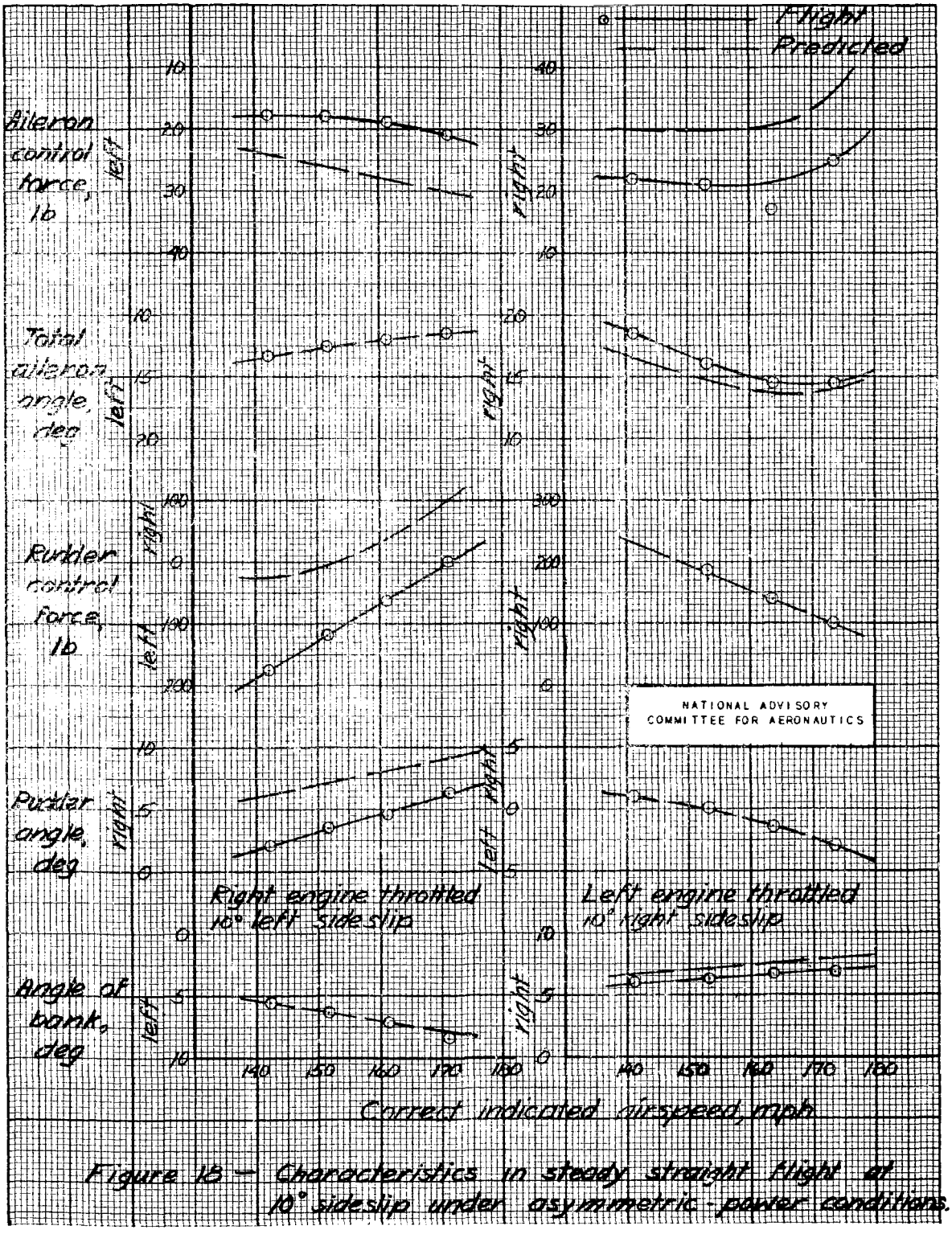

Figure 18 — Characteristics in steady straight flight at 10° sideslip under asymmetric-power conditions.

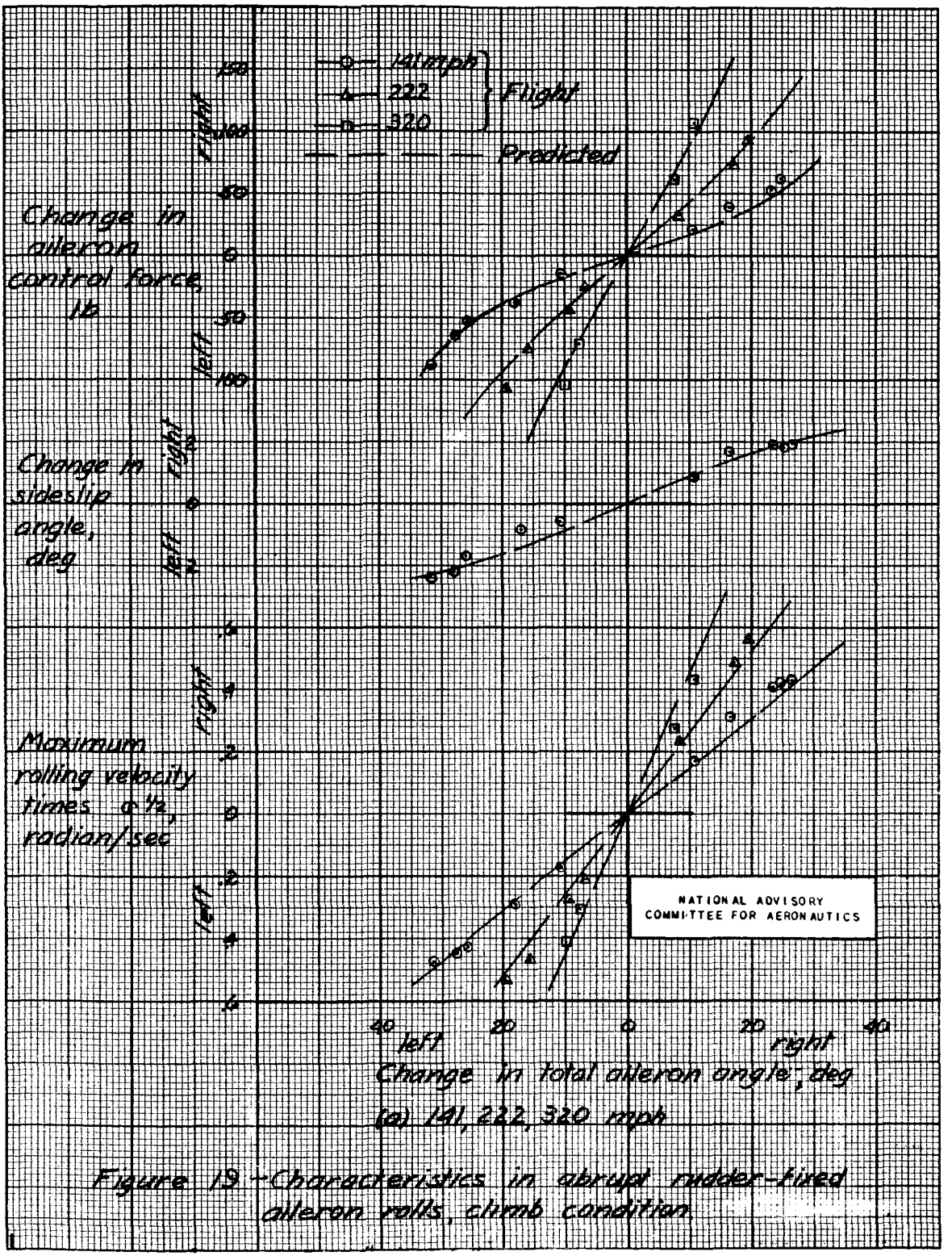

(a) 141, 222, 320 mph

Figure 19.-Characteristics in abrupt rudder-fixed aileron rolls, climb condition.

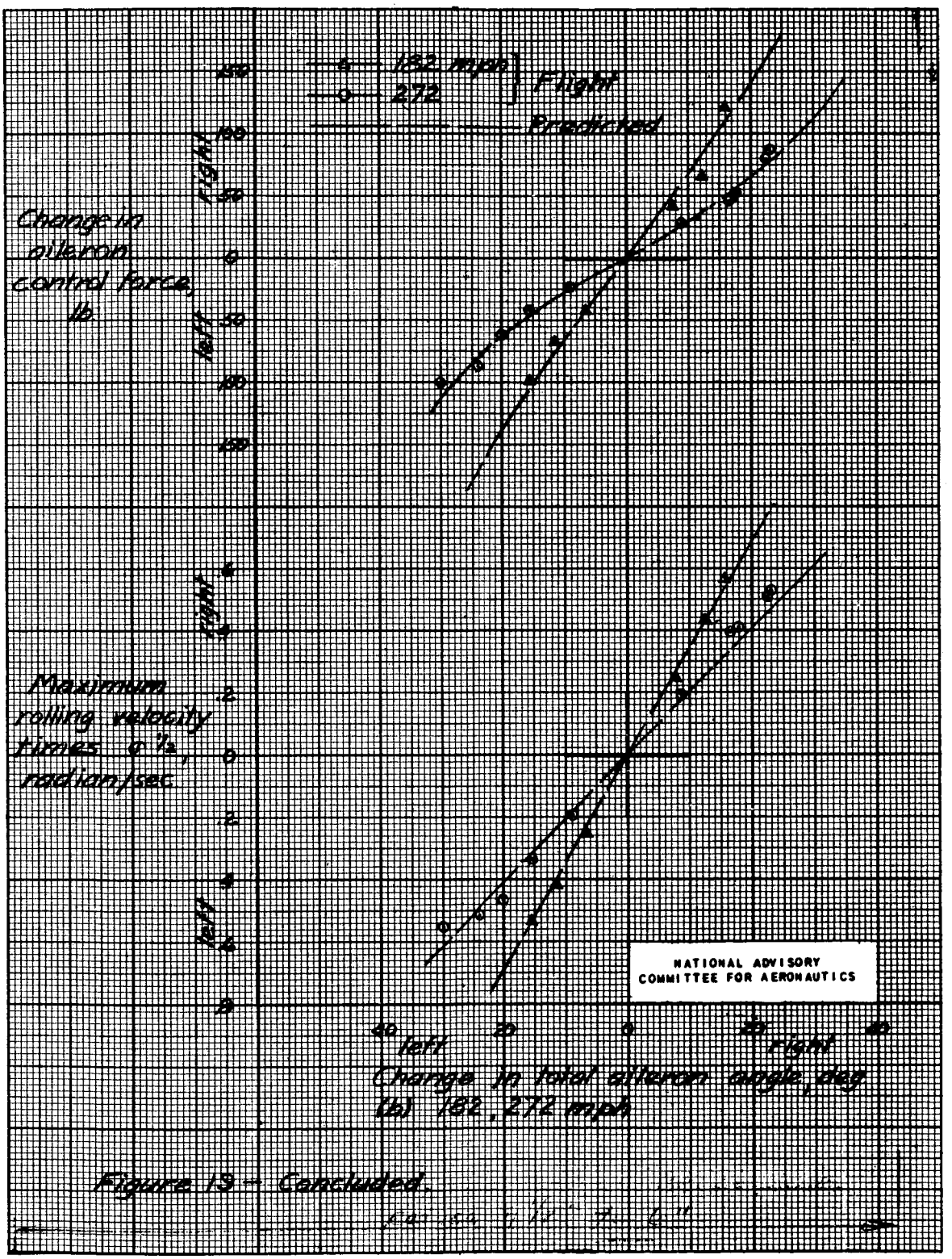

Figure 19 – Concluded.

A71

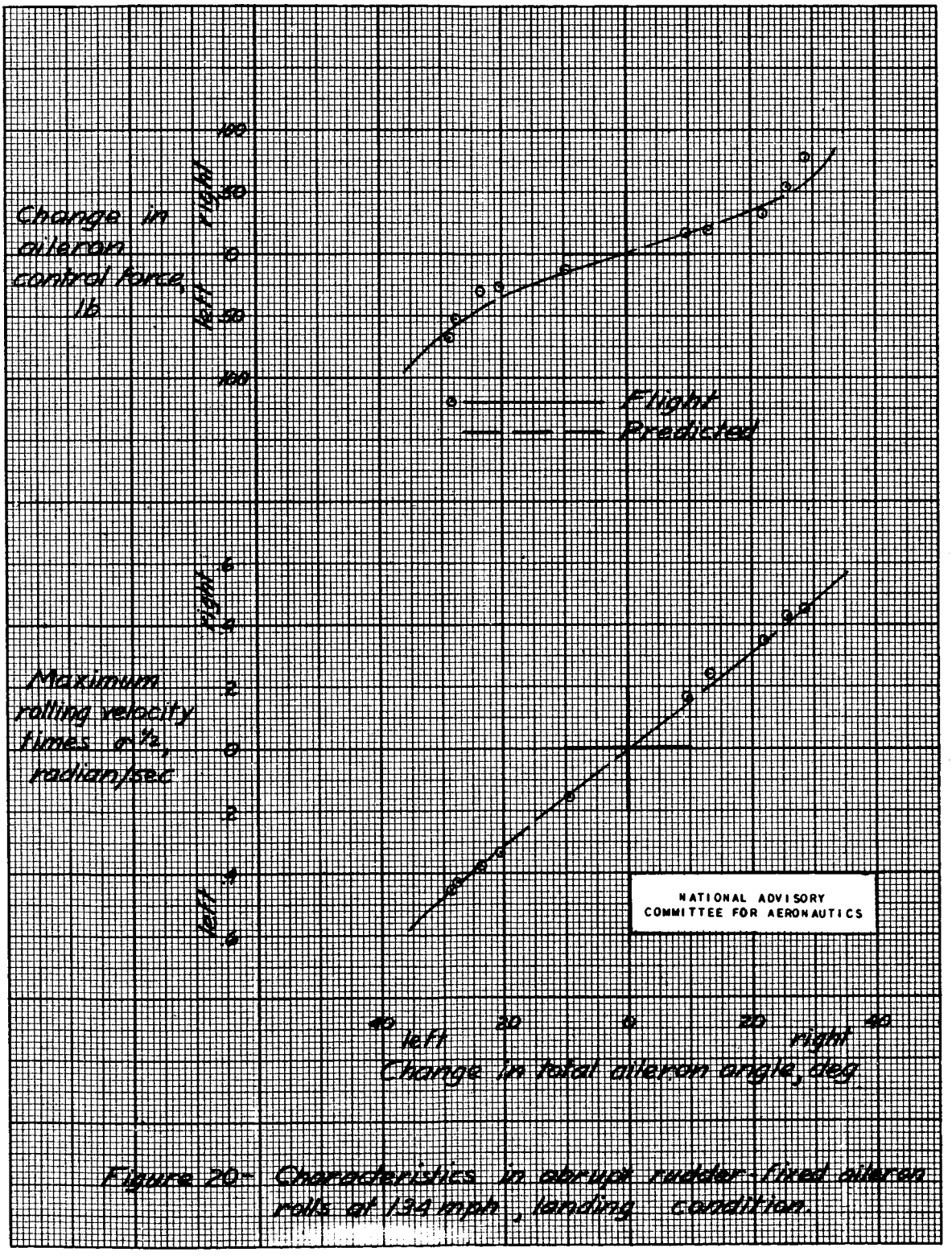

Figure 20.- Characteristics in abrupt rudder-fixed aileron rolls at 134 mph, landing condition.

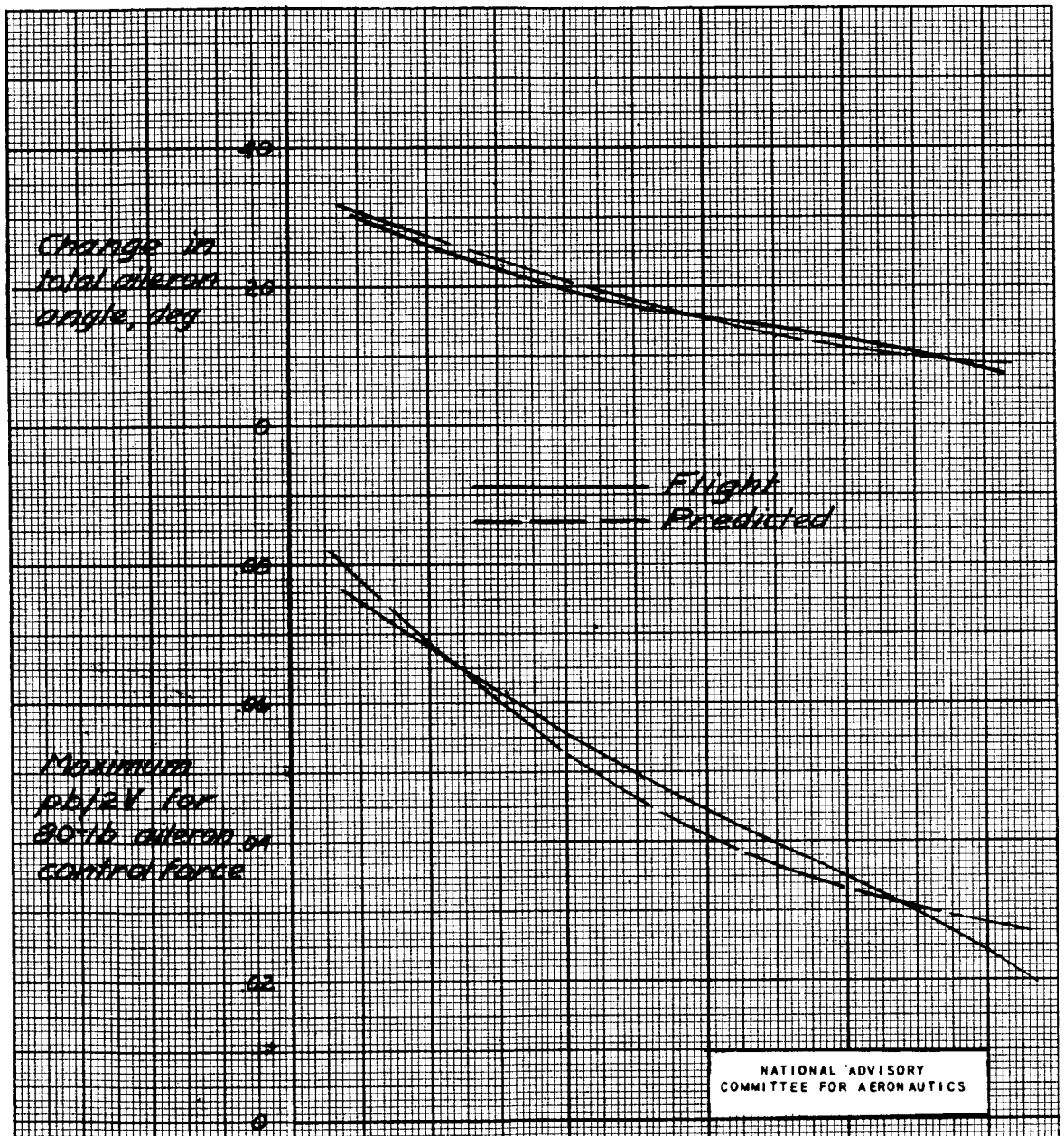

Figure 21 - Variation with indicated airspeed of maximum pb/2V and change in total aileron angle for an 80-pound aileron control force, climb condition.